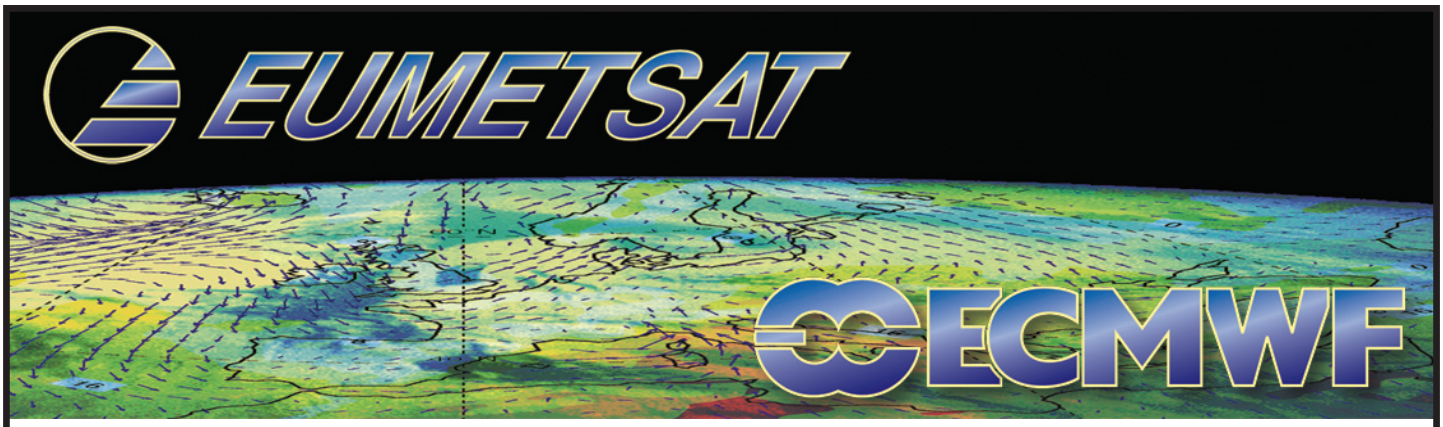

EUMETSAT/ECMWF Fellowship Programme
Research Report No. 46

Indian Ocean AMVs: Moving to Meteosat-8 and assessing alternative options

K. Lean and N. Bormann

Jan 2018

Series: EUMETSAT/ECMWF Fellowship Programme Research Reports

A full list of ECMWF Publications can be found on our web site under:
http://www.ecmwf.int/publications/

Contact: library@ecmwf.int

European Centre for Medium Range Weather Forecasts
Shinfield Park, Reading, RG2 9AX, England

Contents

Executive summary

On 1st February 2017, EUMETSAT approved the move from Meteosat-7 to Meteosat-8 as the primary Indian Ocean Data Coverage (IODC) service. Now in this new location, Meteosat-8 was the natural choice for the replacement of the Meteosat-7 Atmospheric Motion Vector (AMV) and Clear Sky Radiance (CSR) products in the ECMWF operational system. The switch means changing to a newer generation satellite leading to a significant increase in the amount of data available for the IODC in both products and, using Meteosat-10 as an example of the newer generation, better data quality was also anticipated. The first part of this report focuses on the analysis of Meteosat-8 AMVs, initially looking at first guess departure statistics that show the expected improvement over Meteosat-7, such as reducing negative speed biases at high levels in the extra-tropics. Data quality was, reassuringly, very similar between Meteosat-8 and Meteosat-10. Assimilation experiments tested the longer term impacts of the new dataset in the forecast system. These revealed continued benefit of the IODC with positive impacts on the vector wind field at high levels and small reductions in the standard deviations of the fit of conventional wind observations and humidity sensitive observations to the model backgrounds.

The second part of this report investigates potential options for the IODC beyond Meteosat-8. Here we inter-compare a selection of satellites - Meteosat-8, Indian National Satellite - 3D (INSAT-3D) and Feng-Yun-2E (FY-2E) - operated by different centres and consider their relative benefits or limitations. First guess departure statistics are used to understand the data quality and show that the variation in instruments and AMV derivation methods lead to relatively large differences in the values and spatial patterns of the statistics. INSAT-3D overall showed the best agreement with the first guess but this could be explained by a larger dependence of NWP information in the wind derivation. Despite the differences between the datasets, impacts on the forecast system were surprisingly very consistent. For completeness, the benefit of the All Sky Radiances (ASRs), available for Meteosat-8 only, was also considered with assimilation experiments showing positive impacts on the fit of independent humidity sensitive observations to the model background.

During the first experiments conducted for the switch from Meteosat-7 to Meteosat-8 an unexpected area of apparent degradation at 850hPa was found in the middle of the Indian Ocean. Part 3 of the report considers this feature in more detail. The area was also found to be affected by model bias leading to doubt that this was an entirely observation based issue. More thorough investigation was carried out with aid of the other IODC satellites which has highlighted some potentially suspicious behaviour in the low level winds where the wind speed of the AMVs varies little with height compared to the model. Sparse conventional observations coupled with evidence that it is also challenging area for model have made it difficult to make firm conclusions about the truth.

Table 1: Instrument details for Meteosat-7 and Meteosat-8. (IR = Infrared, Vis = Visible, WV = Water Vapour)

	Meteosat-7	Meteosat-8
Position	57.5°E	41.5°E
Imaging instrument	MVIRI	SEVIRI
Channel wavelengths for AMVs (μm)	IR (11.5) Vis (0.70) WV1 (6.4)	IR (10.8) Vis (0.64) WV1 (6.25) WV2 (7.35)
Time frequency of AMVs	1.5 hourly	1 hourly
Pixel resolution (at sub-satellite point)	2.5km (Vis), 5km (IR and WV)	3km
Time between full disc images	30 mins	15 mins

Part I

Replacing Meteosat-7 with Meteosat-8 over the Indian Ocean

1 Introduction

At ECMWF, five geostationary satellites provide the AMV and CSR (or in some cases ASR) coverage in the tropics and mid-latitudes. The loss of any of these would leave a substantial gap in the coverage. The geostationary satellite, Meteosat-7, has provided the IODC service for many years with Atmospheric Motion Vectors (AMVs) and Clear Sky Radiances (CSRs) both actively assimilated at ECMWF from February 2007. As Meteosat-7 reached the end of operational life, Meteosat-8 was drifted across to a new position arriving at 41.5°E in September 2016 and AMVs received from 20th October 2016. Data from Meteosat-7 continued in parallel until the end of March 2017. Both products were successfully switched to Meteosat-8 in the operational system on 2nd March 2017. In this first part of the report we will focus on the replacement of Meteosat-7 with Meteosat-8 AMVs. Details of moving from CSRs to the Meteosat-8 ASR product can be found separately in Letertre-Danczak (In progress).

The change has meant a progression from using a first to second generation Meteosat satellite. Meteosat-7 carried the Meteosat Visible Infra-Red Imager (MVIRI) instrument from which AMVs were derived from three channels while Meteosat-8 satellite carries the Spinning Enhanced Visible Infra-Red Imager (SEVIRI) which provides four channels for AMV derivation. Some of the instrument features relevant for AMVs have been summarised in table 1. The increase in the number of channels and better spatial and temporal resolution results in a large rise in the number of AMVs available. For example, the total daily number of AMVs from the infrared channel on Meteosat-7 varies between around 3.3-3.8x10^4 throughout December 2016 while on the equivalent channel on Meteosat-8 the daily total is 4.4-5.0x10^5. Figure 1 shows the change in position of the IODC and also illustrates the higher density in AMVs.

Assessment of the data quality of Meteosat-8 is made by comparing first guess departures with Meteosat-7 and also Meteosat-10. Due to the positioning of the orbit 16.5° further west there is more overlap between Meteosat-8 and -10. As both carry the same instrument and have the same AMV processing, finding similar data characteristics would provide confidence in the new IODC. To test the longer term

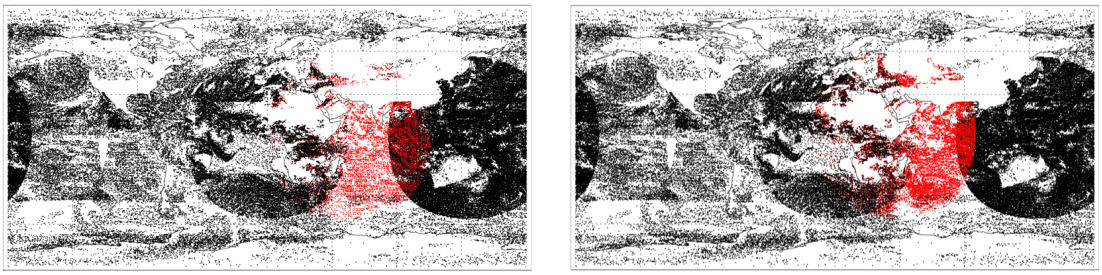

Figure 1: Maps showing the location of AMVs available for active assimilation for 00Z 25th October 2016 when using Meteosat-7 (left) and Meteosat-8 (right). The IODC service has been highlighted in red in both cases.

impacts on the forecast system, assimilation experiments are conducted.

Section 2 describes the quality assessment using first guess departure statistics which compares Meteosat-7,-8 and -10. Results of the assimilation experiments are discussed in section 3. Finally a summary of the switch to Meteosat-8 is presented in section 4.

2 Initial quality assessment

The data quality assessment uses first guess departure statistics for a five week period over 21st Oct - 25th Nov 2016. Here statistics are calculated using the difference between observation and the model background (12 hour short range forecast from the previous model run). The model backgrounds were provided by experiments using a reduced resolution version ($T_{Co}399$ (55km)) of cycle 43r1 of the model which was the operational system at the time. Two different experiments were run: the first with Meteosat-7 actively assimilated as operationally and in the second, Meteosat-7 has been removed and replaced with Meteosat-8 actively assimilated with the same quality control configuration as Meteosat-10 (detailed later in section 3).

2.1 Dependence on Quality Indicator

Meteosat-7, -8 and -10 are all provided with forecast dependent and forecast independent Quality Indicator (QI) values. Usually the forecast independent values are preferred for data screening to avoid aliasing in Numerical Weather Prediction (NWP) information from the data provider (Holmlund, 1998). For Meteosat-7, the forecast dependent value is used operationally as a result of historical reasons - the early data were only provided with the forecast dependent value (e.g. Payan and Rabier (2004)). When the forecast independent values were introduced, the screening process remained unchanged. For Meteosat-10, the forecast independent QI has been used operationally.

Figure 2 shows the dependence of the Root Mean Square Vector Difference (RMSVD) on the forecast independent QI for the high level infrared winds (pressure $<$ 400hPa) in the Northern Hemisphere (latitude $>$ 20°N). This example is representative of the majority of other channels, geographical regions and heights and illustrates the similarity in trends for Meteosat-8 and -10 with RMSVD improving as the QI increases. Meteosat-10 has a larger number of the highest QI values which may be related to the different geographical coverage. For Meteosat-7 the RMSVD for QI values higher than 60 smoothly

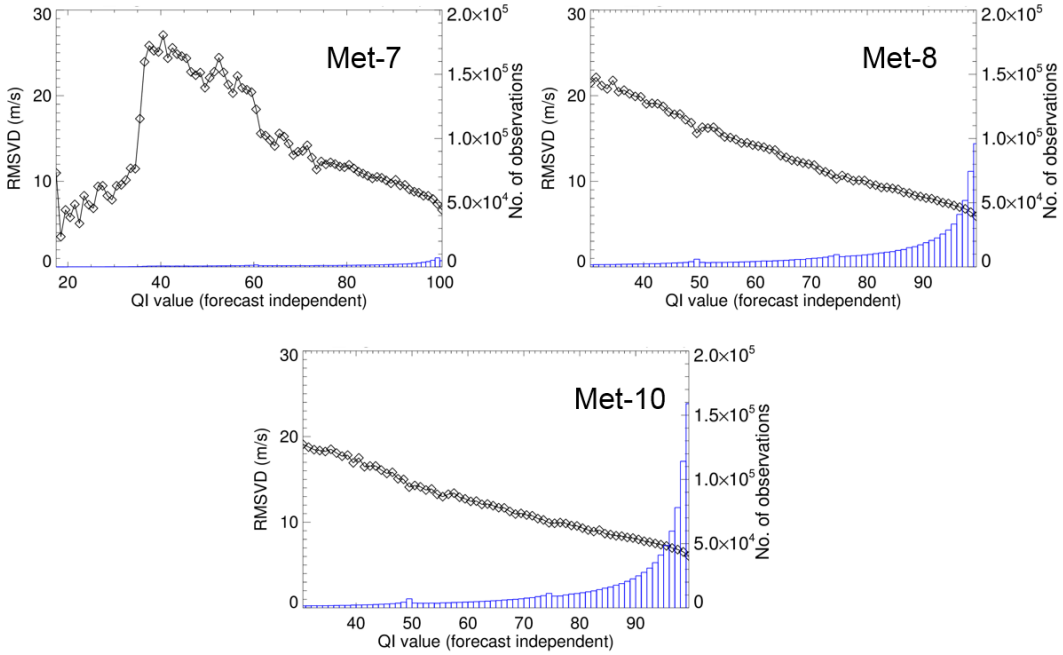

Figure 2: Dependence of RMSVD on forecast independent QI for high level (pressure $<$ 400hPa) and Northern Hemisphere (latitude $>$ 20°N) infrared AMVs from (clockwise from top left) Meteosat-7, Meteosat-8 and Meteosat-10 for 21st Oct - 24th Nov 2016.

decreases but there are large jumps at lower values. Figure 2 also clearly shows the dramatic increase in AMV number between the two satellite generations.

Low levels (pressure $>$ 700hPa) in the Northern hemisphere are an exception where the RMSVD is higher for Meteosat-8 than Meteosat-10 and actually begins to rise again for very high QI values above 90 (not shown). This is likely to be due to differences in geographical coverage with more land present in Meteosat-8 (due to generally poorer statistics, low level AMVs over land are screened from assimilation across all satellites). This pattern of rising RMSVD as QI increases for the very high values is also present in the mid-level AMVs in both Meteosat-8 and -10 for the northern hemisphere and tropics. This behaviour is undesirable but there are far fewer AMVs in this region and the mid-level tropics the data are blacklisted in assimilation.

As the behaviour is very similar between Meteosat-8 and Meteosat-10 for both the quality indicator types, the threshold choices for Meteosat-10 are appropriate to apply to Meteosat-8. All infrared and water vapour AMVs are screened if the forecast independent QI is less than 85 and less than or equal to 85 for the visible AMVs. For comparisons in subsequent statistics, as the independent QI is sensible for high values for Meteosat-7 as well, the same threshold is used for consistency in the preliminary screening when assessing the data quality below.

2.2 Spatial statistics

Latitude/longitude maps and zonal plots of the first guess departure statistics illustrate differences in the horizontal and vertical characteristics of the AMVs. Figure 3 compares the RMSVD, speed bias and

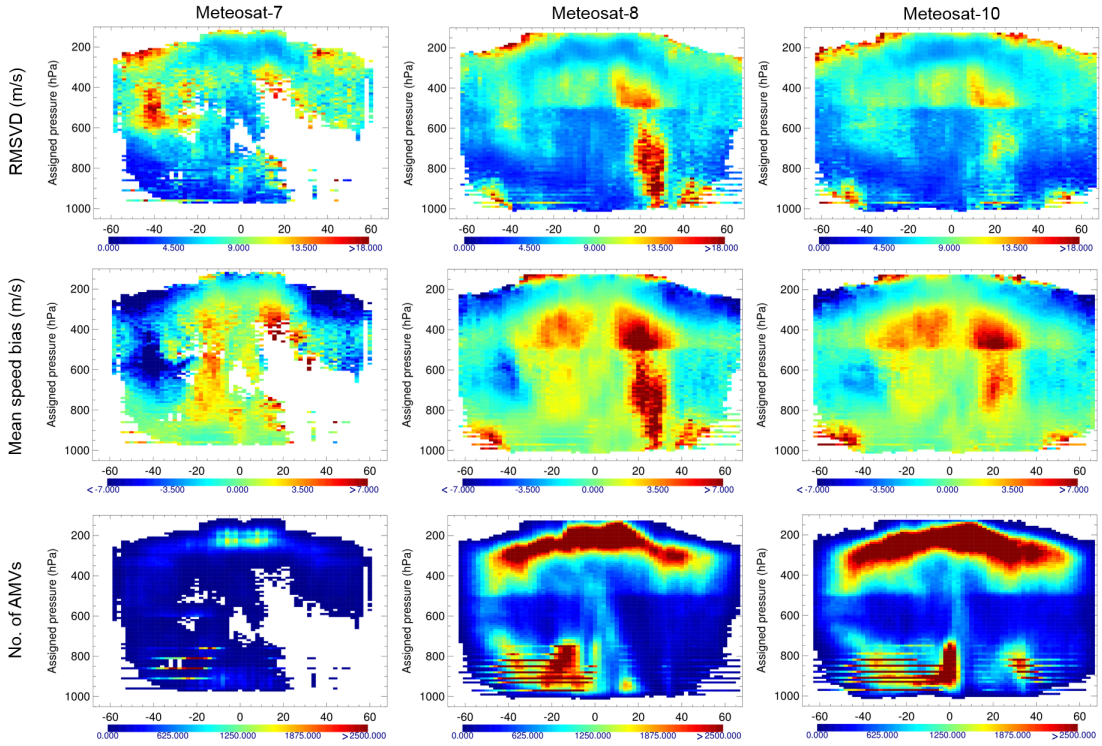

Figure 3: Zonal dependence of RMSVD (top row), speed bias (middle row) and number of AMVs (bottom row) for the infrared channel from Meteosat-7 (left column), Meteosat-8 (centre column) and Meteosat-10 (right column) using data from 21st Oct - 24th Nov 2016. AMVs have been screened using forecast independent QI > 85 and boxes (2° latitude x 10hPa) with fewer than 20 AMVs have also been removed.

number of infrared AMVs for Meteosat-7, -8 and -10. Between Meteosat-7 and -8 there are some clear areas of improvement such as the reduction of the large negative speed bias in the high level, extra-tropics. Overall in the densest areas of AMVs there are lower RMSVD values and smaller speed biases. The number of AMVs is clearly much lower for Meteosat-7 however, the densest areas are in similar locations.

Figure 3 also shows the strong similarity between Meteosat-8 and -10 - the overall patterns and magnitude of values are very close. The good agreement gives confidence that the observations from Meteosat-8 at the new location are sensible. The elevated values around 10-30°N in the low and mid-levels are in an area of very few AMVs (as demonstrated by the area being removed from the Meteosat-7 plot due to insufficient data). The AMVs causing the extreme values are subsequently screened by the first guess check procedure (observations are rejected if the difference from the model background estimate is too large) prior to assimilation. While AMVs from the infrared channel have been used as an example here, conclusions about the high and low level AMVs also apply to the water vapour and visible channels respectively.

Maps of the statistics also supported agreement between Meteosat-8 and Meteosat-10 in the overlap region and general improvement from Meteosat-7. Figure 4 shows an example of the percentage difference (Meteosat-8 minus Meteosat-7) in the overlap region of the RMSVD, the difference in absolute value of speed bias and assigned AMV pressure. Note that these statistics are derived without attempting to first match individual AMVs, so the sampling of the different AMV products may be different. The difference

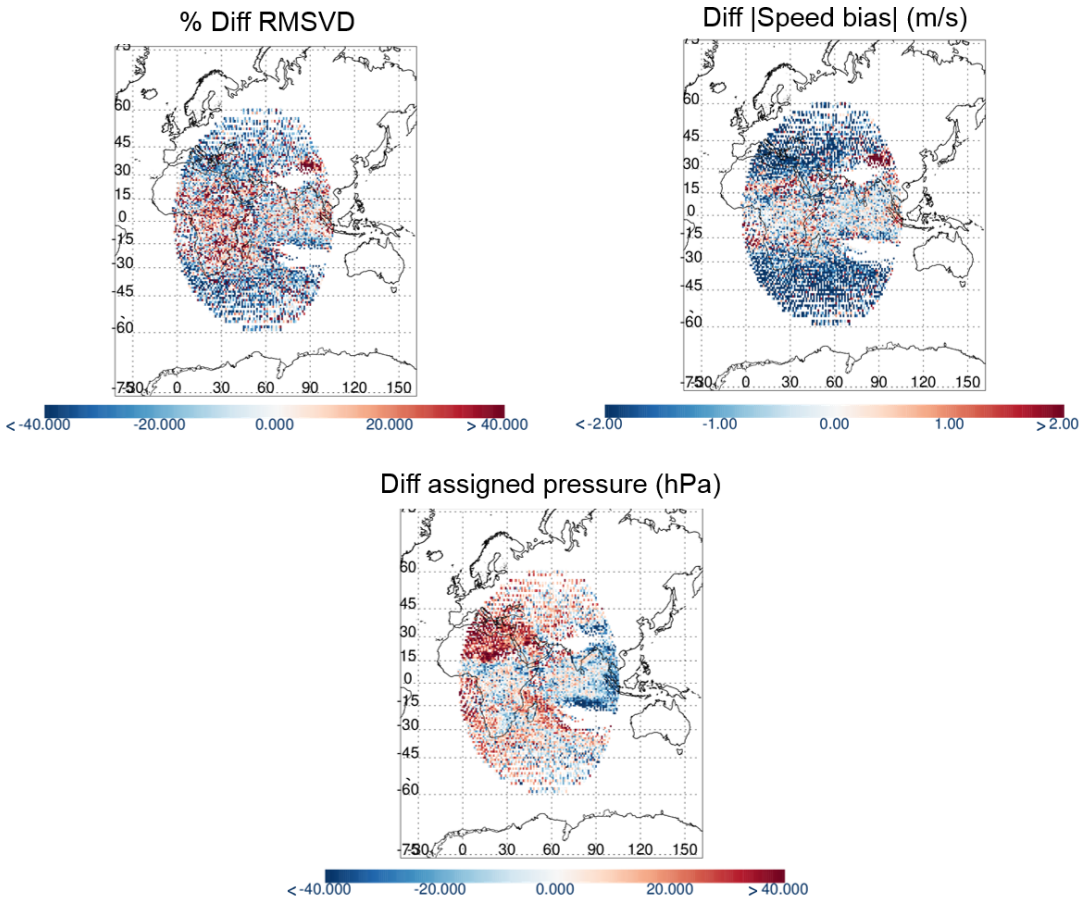

Figure 4: Maps showing the difference between Meteosat-8 and Meteosat-7 statistics for high level (<400hPa) infrared winds. Clockwise from top left: percentage RMSVD from Meteosat-8, difference in absolute value of speed bias, and difference in assigned AMV pressure. Data are from 21st Oct- 24th Nov 2016, QI > 80 and at least 5 matches were required for each box.

in assigned pressure reveals that many of the high level AMVs from Meteosat-8 on the eastern (western) side of the overlap are assigned slightly lower (higher) pressures than Meteosat-7. However, this difference in height has not been detrimental with wide spread improvement of the RMSVD (with the exception of Africa) - much of the area in excess of 20% reduction - and speed biases are closer to zero (indicated by the general blue colour). The positive changes are also found in the water vapour winds, mid-level AMVs and in the tropics at low levels. However, over the ocean in the extra-tropics at low levels, Meteosat-7 shows better agreement with the first guess. Meanwhile, the pattern in assigned pressure is more variable at low levels. For example, in the extratropical infrared winds Meteosat-8 is at a lower pressure (on average by over 40hPa) but the changes in the visible winds is much more mixed for the same region. Differences may occur due to the slightly different wavelengths available on the imaging instrument which will change the height assignment calculations. Further to this, no bias correction is applied prior to height assignment in the EUMETSAT processing. However, the bias characteristics of the water vapour channels changed considerably between Meteosat-7 and Meteosat-8 with a mean bias of 4K in magnitude being reduced to within 0.1K in the first guess departure statistics (Letertre-Danczak, In progress).

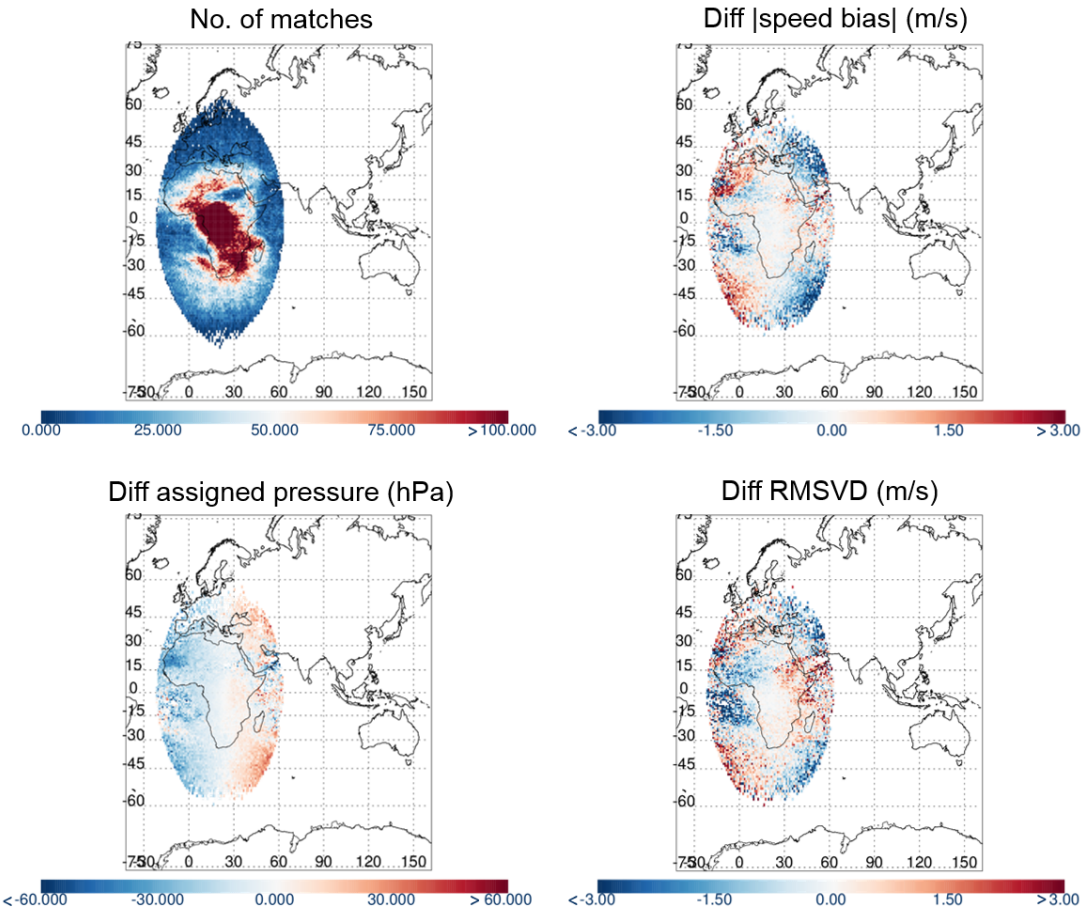

Figure 5: Maps showing (clockwise from top left) the number of matches, difference between absolute values of speed bias, difference in RMSVD and difference in assigned AMV pressure for collocated AMVs (Meteosat-8 - Meteosat-10) for high level (<400hPa) infrared winds. Data are from 1st Nov - 15th Dec 2016 and QI > 80.

When taking the difference between Meteosat-8 and -10, individual AMVs were collocated prior to calculating the statistics to ensure differences are not due to sampling. To do this, AMVs from Meteosat-8 and Meteosat-10 are matched if they are within 0.1° latitude, 0.1° longitude and the same observation time (both AMV products are hourly at half past the hour). High and low level winds were separated so no strict criterion was placed on the pressure apart from restricting matches to be within these broad bands.

Figure 5 shows an east-west divide that suggests that the AMVs at the scan edges, particularly in the extra-tropics, are of lower quality (note this pattern is also present when looking at the difference in active used data). This will be due to the satellites having different orbit positions - at the disc edges the resolution is coarser and also fewer AMVs will be produced. This is highlighting a feature common to both satellites, and it is likely to be a characteristic of AMVs in general. Along the longitude at the centre of the overlap region where the AMV location is roughly equidistant from the centres of both satellites, the difference is reassuringly very small. However, the tropics appears to be exhibiting the opposite behaviour. At the disc edges the assigned pressure of the respective satellite is higher and the magnitude of the speed bias is larger.

Note that the current thinning strategy at ECMWF gives preference to the higher QI value observation if more than one AMV remains in a thinning box after spatial and temporal restrictions have been applied. In the case of Meteosat-8 and Meteosat-10, a simple test selecting the observation to use from the collocation by smallest zenith angle and taking the difference with the statistics when selecting by the highest QI shows a small improvement, especially towards the extremes of the overlap. However, this would be a difficult strategy to use more widely as data quality varies between satellites so zenith angle is no longer a clear indicator. For example, if the two overlapping satellites were of different generations and their derivation processes were less similar, it may be possible in some cases to obtain better quality AMVs at a higher zenith angle of the new satellite than at lower zenith angles of the older satellite.

3 Assimilation experiments

3.1 Set up and blacklisting

As summarised above, the data quality for Meteosat-8 is comparable to Meteosat-10 and improved from Meteosat-7. As the difference in data number and departure characteristics was relatively significant assimilation experiments to test the longer term impact of switching to Meteosat-8 were required. This also allows the opportunity to make sure that sensible quality control choices are made in the screening process prior to assimilation. Experiments were run with a reduced resolution version ($T_{Co}399$ (55km)) of cycle 43r1 of the forecast model. Before assimilation, the AMVs pass through three main quality control steps: blacklisting, a first guess departure check and thinning (200kmx200km, 50-175hPa variable depth boxes, 30 minutes). Due to the similarity between the satellites, the existing channel specific blacklisting choices and observation errors for Meteosat-10 were chosen as the initial configuration to apply to Meteosat-8. Results presented here are from the period 21st Oct 2016 - 7th March 2017. Although the end of March is when Meteosat-7 data distribution ended (with a brief outage for a decontamination from 9th-14th March) decisions regarding the replacement were made at the end of February to allow a more convenient date for the change of satellites to be introduced in the operational system.

Results from early tests revealed degradation in the forecast vector wind fields at low pressures (around 100hPa) particularly affecting the IODC region as well as worsening the fit of independent wind observations to the model background. A similar signal was observed in a previous investigation at ECMWF concerning the introduction of Himawari-8 AMVs (Lean et al., 2016). There are few AMVs at pressures above 150hPa but in moving to the newer generation of Meteosat the relative number is increased significantly (around three times more AMVs assimilated about 100hPa for Meteosat-8 compared to Meteosat-7). It is not clear why including these high level AMVs has a negative impact and it would be interesting to investigate, particularly now the effect has been seen in two different satellites and geographical regions. However, for the purposes of a timely introduction of Meteosat-8, simply screening AMVs with pressures less than 150hPa removed the significant degradation.

Earlier studies also showed a weak but inconclusive signal when using one compared to two water vapour channels on Meteosat-10 (Lean et al., 2016). However, in separate experiments using one (7.35μm) or both water vapour channels for Meteosat-8 the difference in the impact on the forecast system was not significant and there was no clear negative signal by including AMVs from the additional water vapour channel. As there was no clear distinction between using one or two water vapour channels, for consistency with Meteosat-10, a configuration using two water vapour channels was selected.

With the information above, we can construct the channel specific selection for Meteosat-8. Using Meteosat-10 screening choices as a starting point then accounting for the screening of high level winds

and using two water vapour channels, the final experiment for Meteosat-8 allows AMVs as follows:

- Visible channel: Pressure $>$ 700hPa, forecast independent QI $>$ 85
- Infrared channel: forecast independent QI $\geq$ 85, pressure $<$ 150hPa for all latitudes and pressure $<$ 250hPa for $|$latitude$|$ $<$ 25
- Water vapour channel (6.25μm): Cloudy winds only, forecast independent QI $\geq$ 85, 400hPa $\leq$ pressure $<$ 150hPa
- Water vapour channel (7.35μm): Cloudy winds only, forecast independent QI $\geq$ 85, 600hPa $\leq$ pressure $<$ 150hPa for $|$latitude$|$ $\geq$ 25 and 250hPa $<$ pressure $<$ 150hPa for $|$latitude$|$ $<$ 25

These are in addition to screening choices applied in general that reject AMVs with assigned pressures more than 1000hPa or less than 100hPa globally. Over land, AMVs are excluded globally for pressure $>$ 500hPa and at any height over the Himalayas and Northern Hemisphere land above 20°N for longitudes west of 30°E or east of 100°E and north of 35°N for 20°W-30°E. The control for this experiment has the IODC AMVs removed (i.e. no Meteosat-7). A further experiment which reintroduces Meteosat-7 was run in order to allow comparison of the impacts of the two satellites.

3.2 Experiment results

The large scale impacts for the use of IODC AMVs are generally small and close to neutral but there are localised changes seen in the verification against own analysis for the 200hPa vector wind field (figure 6). In an area just south of India there is a reduction in error which is persisting out to forecast lead times of 72 hours. While the feature is present for both Meteosat-7 and -8, it is more prominent and longer lasting for Meteosat-8.

Another important measure of the impact of the data is the change in fit of independent observations to the model background. Reduction in the standard deviation of the first guess fit indicates closer agreement with other observation types through improvements to the model background fields. Over large verification areas often used (e.g. the whole tropics region) the signal from the additional AMVs is lost resulting in mostly neutral results. To get a clearer picture of whether the AMVs are beneficial, a smaller region covering the IODC area (60°N-60°S, 30-120°E) was considered.

Figure 7 shows examples of the changes to radiosonde wind observations and to humidity and temperature sensitive channels on the Advanced Technology Microwave Sounder (ATMS) instrument. The changes for both are largely neutral although there are small indications of positive impact on the wind observations at higher levels, in particular for Meteosat-8 where two adjacent pressure levels in the U component are showing significant changes. However, a slight degradation at 100hPa suggests that over a longer verification period we were not able to completely eliminate the negative effects that resulted in the removal of the very high AMVs described earlier. In the humidity channels on ATMS, impacts are again close to neutral although Meteosat-8 does show two channels that are significant within the 95% confidence levels. Results from the Microwave Humidity Sounder (MHS) instruments on various satellites (not shown) also show improvements in the highest peaking channel. There is also a small degradation for temperature sounding channels 9 and 10 on ATMS shown here. The reasons for this are not fully understood however the degradation is small and not present in equivalent channels on the Advanced Microwave Sounding Unit - A (AMSU-A) instruments so it is not considered a major concern.

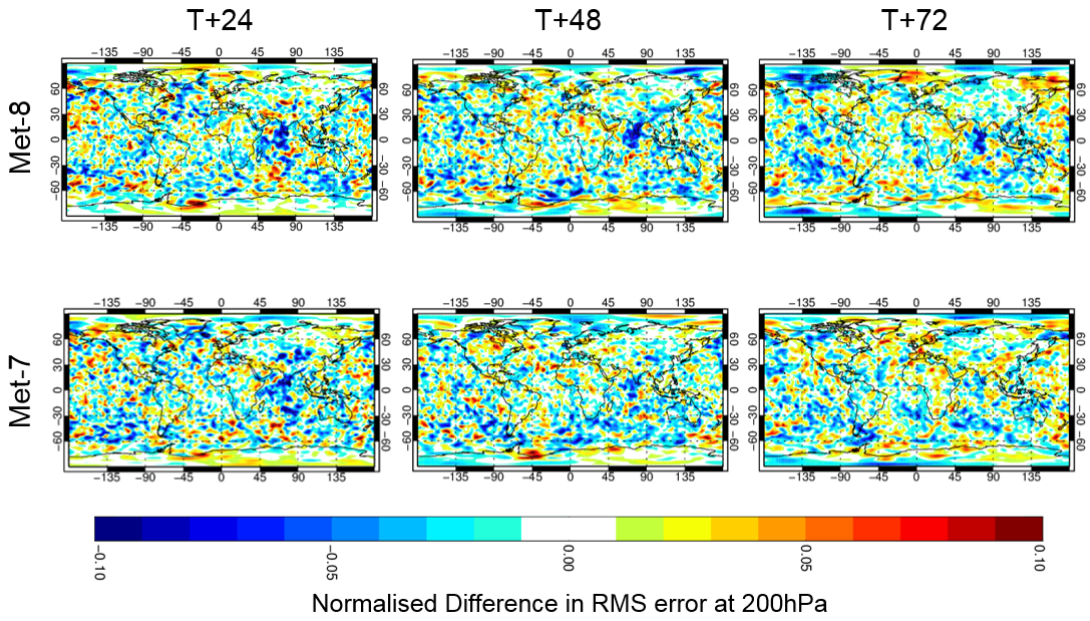

Figure 6: Maps showing the change in vector wind error at 200hPa verified against own analysis for Meteosat-8 (top row) and Meteosat-7 (bottom row) at forecast lead times of 24, 48 and 72 hours (left to right columns). Experiment period is 21st Oct 2016 - 7th Mar 2017.

3.2.1 Feature at 850hPa

Verification against own analysis at lower pressures and independent observation fits do not show anything worrying for the inclusion of Meteosat-8. However, at low levels there is a localised feature showing apparent degradation at 850hPa in the vector wind field verified against own analysis (figure 8). The strength of the feature is somewhat sensitive to the choice of verifying analysis, but some degradation can still be found when verifying, for instance, against the operational analysis. A signal is not seen at low levels in the independent wind observations but the location of this feature in the middle of the Indian Ocean means that few conventional observations are within the affected area. The signal is present but much weaker for Meteosat-7 with the greater data volume for Meteosat-8 allowing more reinforcement of the change. Verification at the surface does not show any systematic negative impacts and fits of the 10m scatterometer winds does not appear significantly changed suggesting the problem is localised around 850hPa.

The feature is most prominent in the early weeks of the experiment and appears to weaken in the latter half of the four months. Further analysis shows that, particularly in the first half of the experiment, the AMVs act to increase the westward flow of the wind in the analysis around the same area (figure 9). At the same time, investigation of the forecast errors in this region show evidence of a model bias where forecast winds are too slow compared to analysis. This model bias may be contributing to the presence of this feature but it cannot be ruled out that the AMVs are also partly responsible. Exploring the characteristics of other IODC satellites (presented in the second part of this report) gave the opportunity for further investigation into this issue. An in-depth discussion of the 850hPa winds, which also covers in more detail the model bias mentioned here, is given in part 3 of this report.

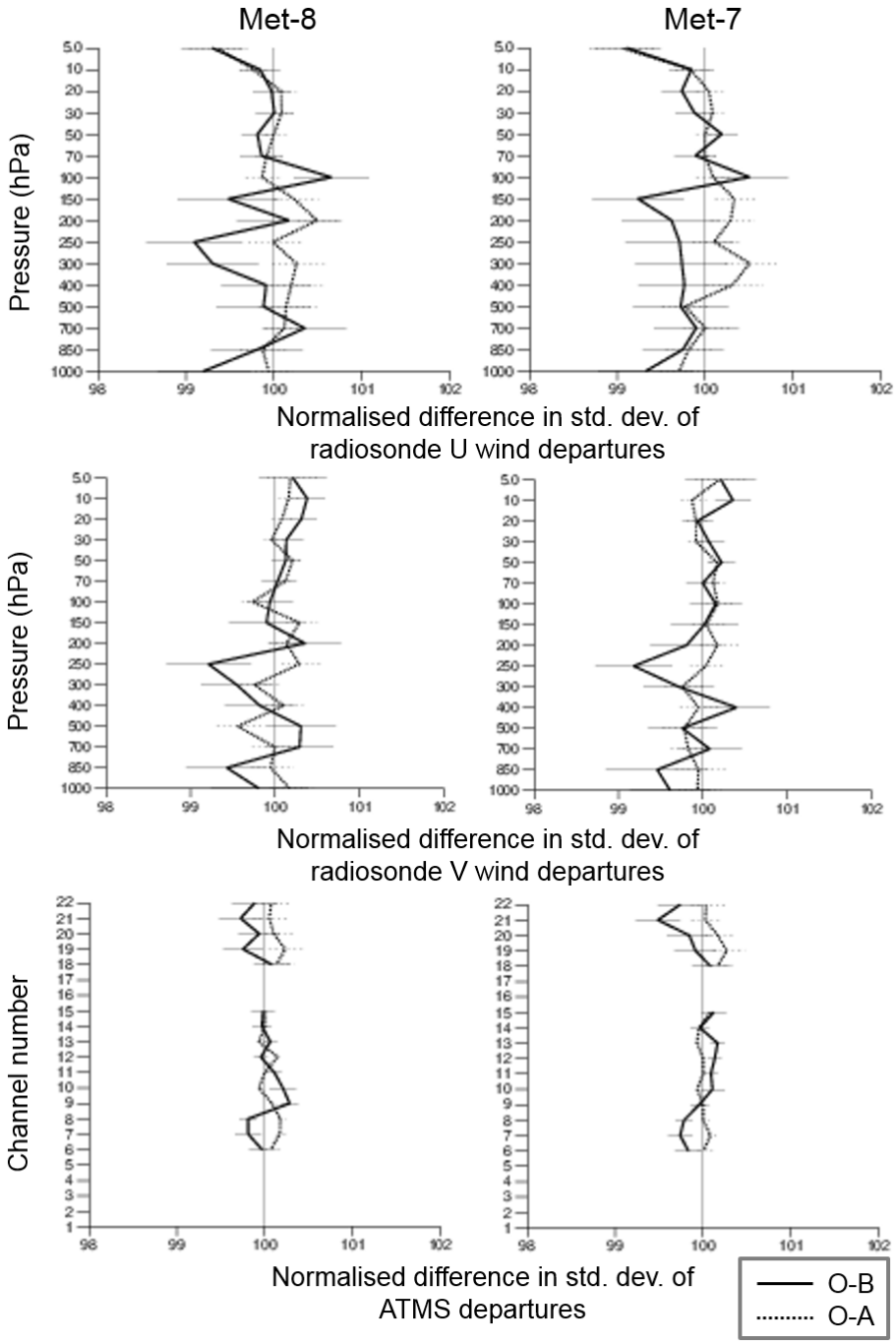

Figure 7: Change in the standard deviation of the fits to background and analysis for the radiosonde U wind component (top row), V wind component (middle) and ATMS (bottom row) over the Indian Ocean region for the Meteosat-8 (left column) and Meteosat-7 (right column) experiments (Data from 1st Nov 2016 - 28th Feb 2017).

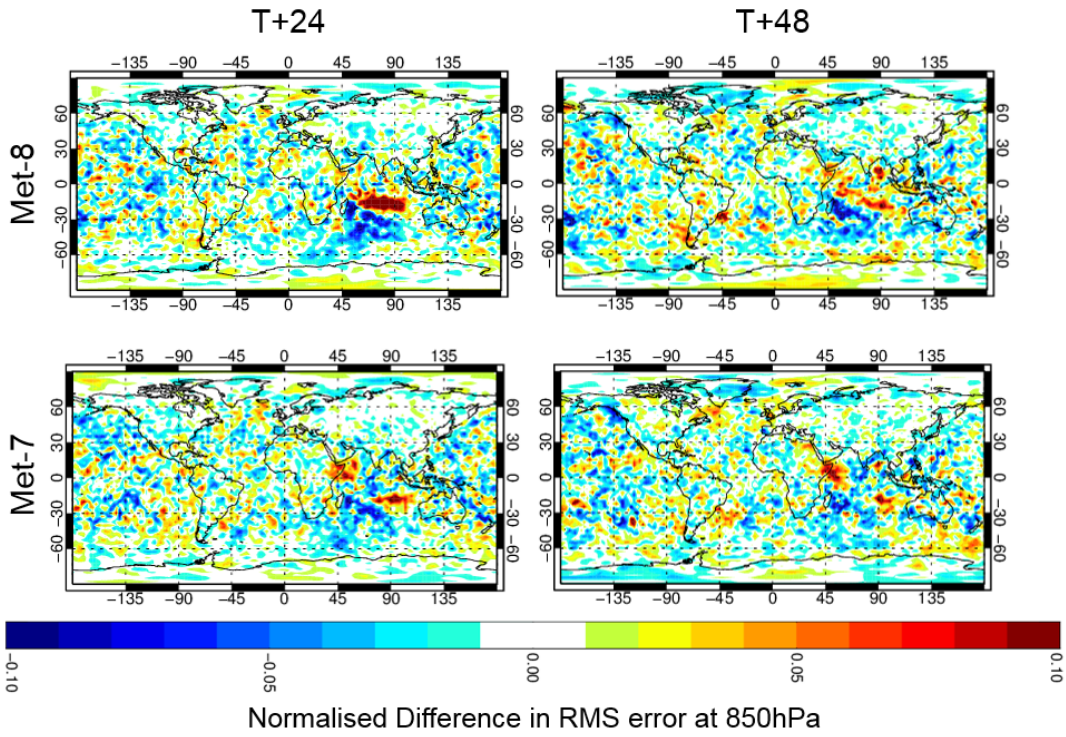

Figure 8: Maps showing the change in vector wind error at 850hPa verified against own analysis for Meteosat-8 (top row) and Meteosat-7 (bottom row) at forecast lead times of 24 (left) and 48 (right) hours. Experiment period is 21st Oct 2016 - 7th Mar 2017.

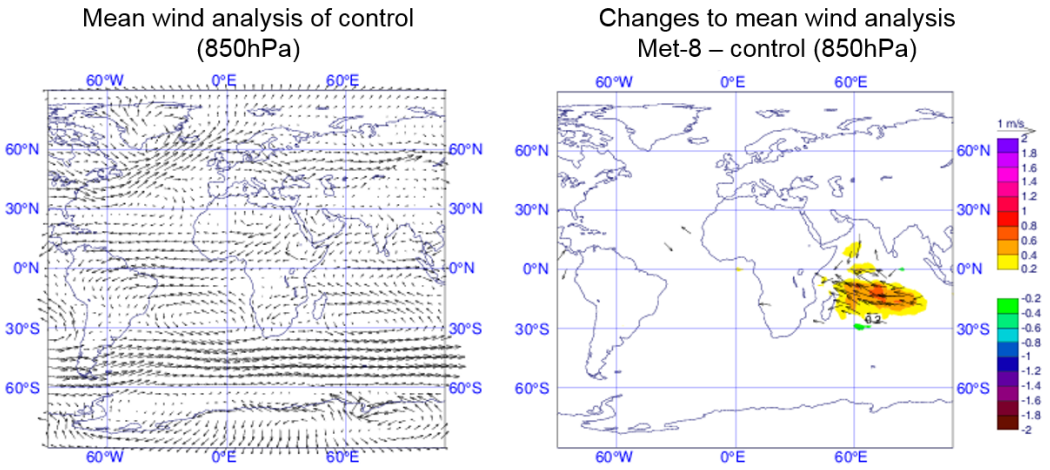

Figure 9: Maps showing the mean wind analysis for the control (left) and the difference in mean wind analysis (right) between the experiment including Meteosat-8 and the control (data from 21st Oct - 18th Dec 2016.)

4 Meteosat-8 conclusions

On 2nd March 2017, Meteosat-8 replaced Meteosat-7 in the operational system as the primary Indian Ocean geostationary satellite. By moving to a second generation satellite many more AMVs became available and data quality was improved including reduction of the large negative speed biases in the extra-topics. As expected, there is a very close agreement in terms of departure statistics between Meteosat-8 and Meteosat-10 which theoretically have the same instrument and derivation method. Analysis of the overlap region revealed the AMV characteristics changed with distance from the satellite nadir point. AMVs located closer to their respective disc centre were assigned a higher pressure which lead to generally smaller speed biases and lower RMSVD values.

Assimilation experiments comparing the impact of Meteosat-8 and Meteosat-7 to a control with no IODC AMVs showed benefit in the verification at high levels. The error in vector wind field at 200hPa was reduced over the Indian Ocean and small but significant changes where seen in the conventional wind observations and two of the humidity sensitive ATMS channels in the area most directly affected by the data. Otherwise, changes were largely neutral apart from an area of apparent degradation at 850hPa in the tropics when verification against own analysis is considered. It transpired to also be a difficult region for the model wind fields with evidence of model biases. The use of the AMVs in the affected area has remained unchanged and further discussion of the issue can be found in part 3 of this report where comparison with other IODC satellites is also made.

Part II

Further IODC options

5 Introduction to IODC satellites

Results presented in the previous section demonstrated that the IODC service provides benefit to the NWP system. The aim of this investigation is to evaluate potential options for the IODC beyond Meteosat-8. Here we will inter-compare a selection of satellites operated by different centres where first guess departure statistics will be used to understand the data quality followed by assimilation experiments to test the longer term impacts of using different datasets in the forecast system.

At the time of investigation, in addition to Meteosat-8, satellites whose coverage extends over the Indian Ocean are INSAT-3D (operated by the Indian Meteorology Department (IMD)) and two Chinese satellites, FY-2E and FY-2G (operated by the China Meteorological Administration (CMA)). Of the Chinese satellites, FY-2G is slightly further east which means that the gap between Himawari-8 and Meteosat-10 is less well covered. Subsequent data quality analysis revealed that FY-2E and FY-2G have very similar characteristics so the decision was made to only continue testing with FY-2E. Conclusions from FY-2E should also be broadly applicable to FY-2G but the slight shift in coverage means that impact should be greater for FY-2E. Figure 10 shows the coverage of the final three IODC services used for this study.

An earlier study was carried out at ECMWF regarding Indian Ocean AMVs (Salonen and Bormann, 2015) which considered Meteosat-7, FY-2E and INSAT-3D. Results showed that the Chinese and Indian satellites showed promise but limitations at the time of testing (such as water vapour AMVs from FY-2E were not separated into clear and cloudy situations) meant that Meteosat-7 was seen to still have a slight

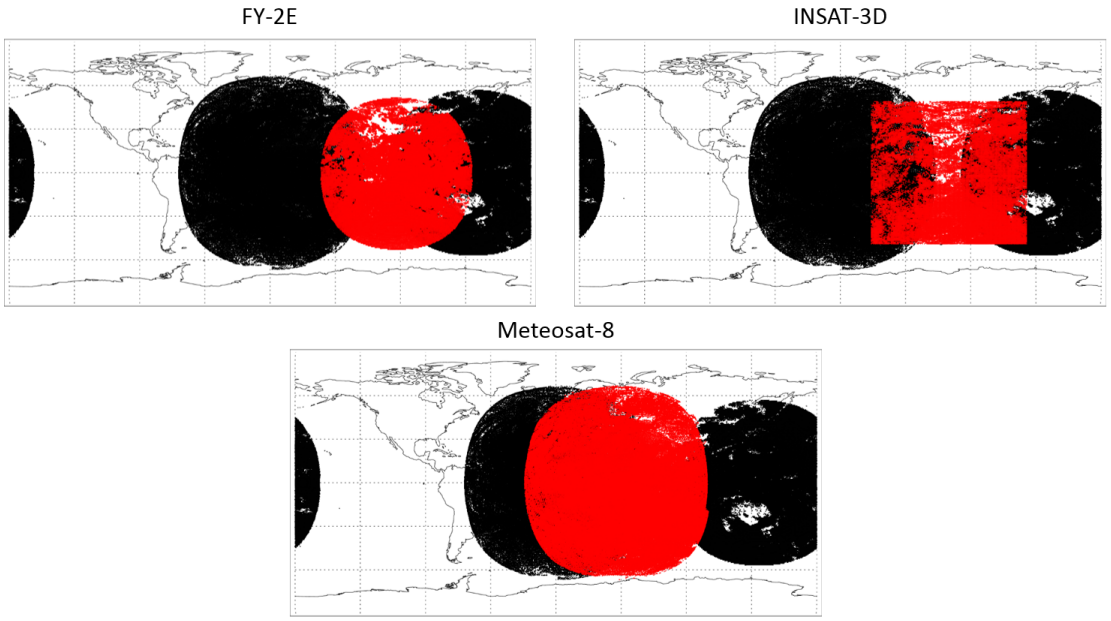

Figure 10: Maps showing the location of the different potential IODC providers additional to Meteosat-8 and the adjacent operationally used geostationary satellites (Meteosat-10 and Himawari-8) using all AMVs from 00Z 25th Oct 2016. Clockwise from top left: FY-2E, INSAT-3D and Meteosat-8. The IODC service has been highlighted in red in each case.

advantage. Due to data availability during the time period of testing, INSAT-3D was not included in the assimilation experiments. Since this investigation, improvements have been made including separation of clear-sky and cloudy water vapour winds on FY-2E and Meteosat-8 is now new to the inter-comparison. Findings from this earlier work were used as guidance for analysis but we will update the results with impacts from any developments in the past two-three years and the addition of INSAT-3D and Meteosat-8.

While the primary focus of this study is the AMVs, when assessing the relative benefits of the different IODC satellites for completeness we must also consider the impact from CSR/ASR products. At ECMWF, we directly assimilate CSR/ASR products and have found clear positive impact from their inclusion (e.g. Lupu and McNally (2014)). Both INSAT-3D and FY-2E/-G do not currently have an ASR or CSR product which was noted as a disadvantage in the earlier study by Salonen and Bormann (2015). When looking at the overall value in NWP of observations assimilated from each IODC satellite we will also make an effort here to account for both AMVs and radiances.

Each AMV production centre has a different technique for deriving the AMVs and there are also differences in the imaging instruments leading to a range in spatial and temporal resolution. Section 6 summarises the key characteristics of each satellite including a discussion of the various AMV algorithms. A data quality analysis carried out through use of first guess departure statistics is presented in section 7. Section 8 examines the impact of the different satellites in the assimilation system. A summary of the findings and thoughts on the future options for IODC are discussed in section 9.

Table 2: Instrument details for Meteosat-8, FY-2E and INSAT-3D. (IR = Infrared, SWIR = Short wavelength IR, Vis = Visible, WV = Water Vapour)

	Meteosat-8	FY-2E	INSAT-3D
Position	41.5°E	86.5°E	82.0°E
Imaging instrument	SEVIRI	S-VISSR	IMAGER
Channel wavelengths for AMVs (μm)	IR (10.8) Vis (0.64) WV1 (6.25) WV2 (7.35)	IR (10.8) WV1 (6.8)	IR (10.8) SWIR (3.9) Vis (0.65) WV1 (6.9)
Time frequency of AMVs	1 hourly	6 hourly	30 minutes
Pixel resolution	3km	5km	1km (Vis), 4km (SWIR/IR), 8km (WV)
Availability after Met-8 moved to IODC	From 20th Oct 2016	From 1st Dec 2016 (WV not separated into clear/cloudy before)	No restrictions

6 Satellite details and derivation methods

The IODC satellites have different imaging instruments from which the AMVs are derived and also have slight restrictions on the time period for study (summarised in Table 2). The result of the differences in numbers of channels, resolution and time frequency means that there is a significant variation in the number of AMVs available. Figure 11 illustrates the daily totals of AMVs from each channel on the three satellites showing that Meteosat-8 has the highest number of AMVs in total and for equivalent channels. It also highlights that the daily number of AMVs is quite stable for both Meteosat-8 and FY-2E while there is a lot of day to day variability for INSAT-3D and even a short complete outage. In a longer time series (not shown) this variability appears to be quite usual and there have been a small number (around 6) of short outages each at least 24 hours in the past 18 months.

As well as different instrument characteristics, there are different AMV derivation methods employed for each satellite. A short summary of each satellite is given here, particularly to provide the key points for the height assignment processes, while further detail can be found in their respective references.

6.1 Meteosat-8 algorithm

Details of the Meteosat derivation scheme can be found in MSG Meteorological Products Extraction Facility Algorithm Specification Document (2015). For Meteosat-8, four consecutive images are used in the tracking step. After selecting an appropriate target the height assignment is based on the Cloud Analysis (CLA) scheme to obtain the cloud height and Cross-Correlation Contribution (CCC) method to apply the results to appropriate pixels in the target. The cloud heights produced by CLA are based on the ratio methods used in CO_2 slicing (Menzel et al., 1983) and H_20 intercept (Szejwach, 1982). However, instead of two channels alone, the final pressure may be a combination of the ratios calculated using the

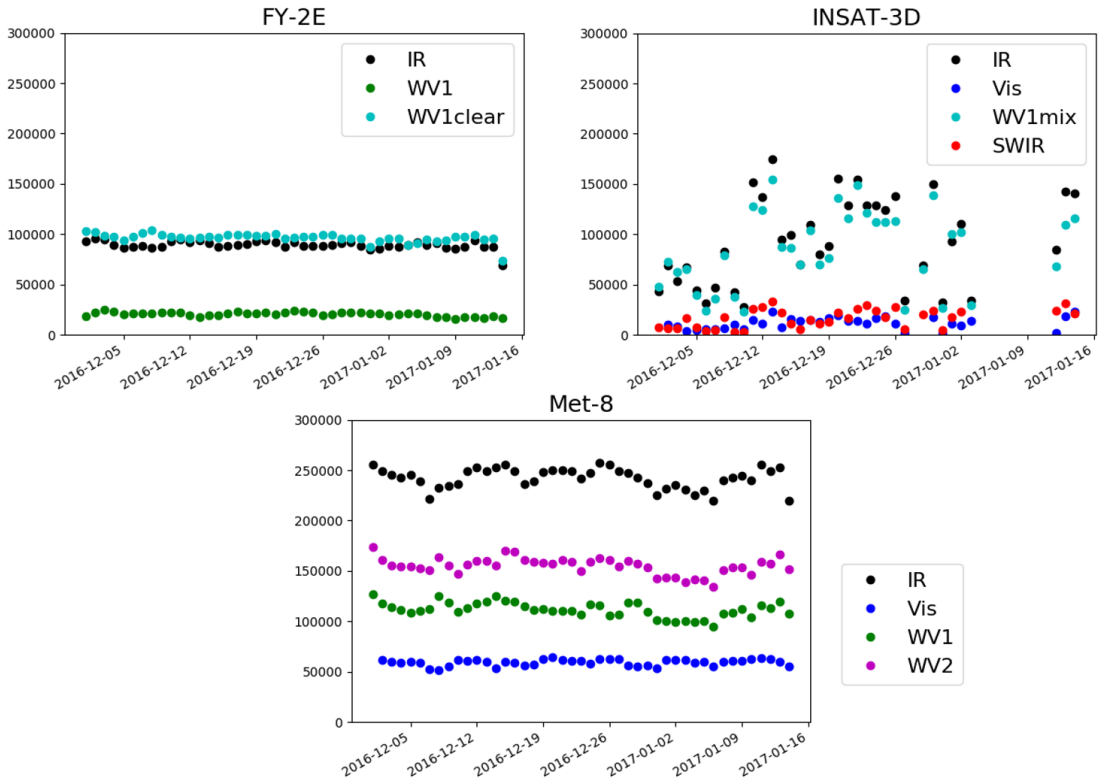

Figure 11: Time series of daily totals of all AMVs available for each channel on FY-2E (top left), INSAT-3D (top right) and Meteosat-8 (bottom) for 1st Dec 2016 - 14th Jan 2017.

following pairs: 13.4μm and 10.8μm, 6.2μm and 10.8μm, 7.3μm and 10.8μm. An inversion scheme is also in place such that if an inversion is detected at a pressure larger than the CLA calculated pressure, the final AMV is reassigned to the lower height of the inversion. The use of NWP profiles in the inversion calculation means that certain pressure levels (corresponding to model levels) are favoured for the height assignment when corrections are applied.

6.2 FY-2E algorithm

The FY-2E scheme (Xu et al., 2002) uses three consecutive images in the tracking. It is worth noting that the speeds are given only in whole numbers of metres per second whereas most other AMV producers use a precision of at least one decimal place. Height assignment for opaque clouds uses the Equivalent Blackbody Temperature (EBBT) technique (Nieman et al., 1993) while using a method based on the H_2O intercept technique for semi-transparent clouds. Pixel selection for the height assignment is also based on the CCC method employed for Meteosat-8. Corrections are often applied to the height of semi-transparent clouds, more common for high level clouds, by using the relationship between the water vapour and infrared EBBTs.

An inversion scheme is also in place (Zhang et al., 2016). The surface temperature under clear sky is important in the normal height assignment technique. However, in the presence of an inversion the surface points are no longer the warmest which prevents the surface temperature from being estimated in the same way as for other situations. To determine the clear sky surface temperature in the image for these inversion cases, the warm pixels from the inversion must first be excluded. The surface temperature is then obtained by constructing a linear relationship between the water vapour and infrared temperatures using the remaining points.

6.3 INSAT-3D

The tracking step of INSAT-3D spans more images than traditionally used by other geostationary satellites (Deb, 2012). A minimum of five consecutive images are required and if present, up to nine images are considered (which would span up to 240 minutes). The large number of images are justified in Deb (2012) as maintaining a minimum decorrelation timescale during retrieval. For the height assignment, the processing follows the GOES-13/-15 derivation (e.g. Velden et al. (1998); Deb et al. (2016)) which uses similar techniques to the other satellites such as CO_2 slicing and water vapour intercept methods. Then there is also the addition of an auto-editor (Deb (2012), pers. comm. S. Deb, Indian Space Research Organization) where many heights are recalculated based on minimising a cost function that combines the observations with first guess forecast values within 50hPa limits. This results in more dependence on the forecast information and the AMV heights favour a set of regularly spaced pressure levels. No inversion correction is applied to the data.

7 Data quality analysis

Salonen and Bormann (2015) showed that the data quality of INSAT-3D and FY-2E was comparable to Meteosat-7. However, it was suggested that future improvements would be the separation of cloudy and clear sky scene in the water vapour channels and more meaningful quality information. Since this earlier work, FY-2E AMVs now follow the recommendation for the water vapour channel and are provided with associated forecast independent QI values. The first guess departure data quality shows a meaningful

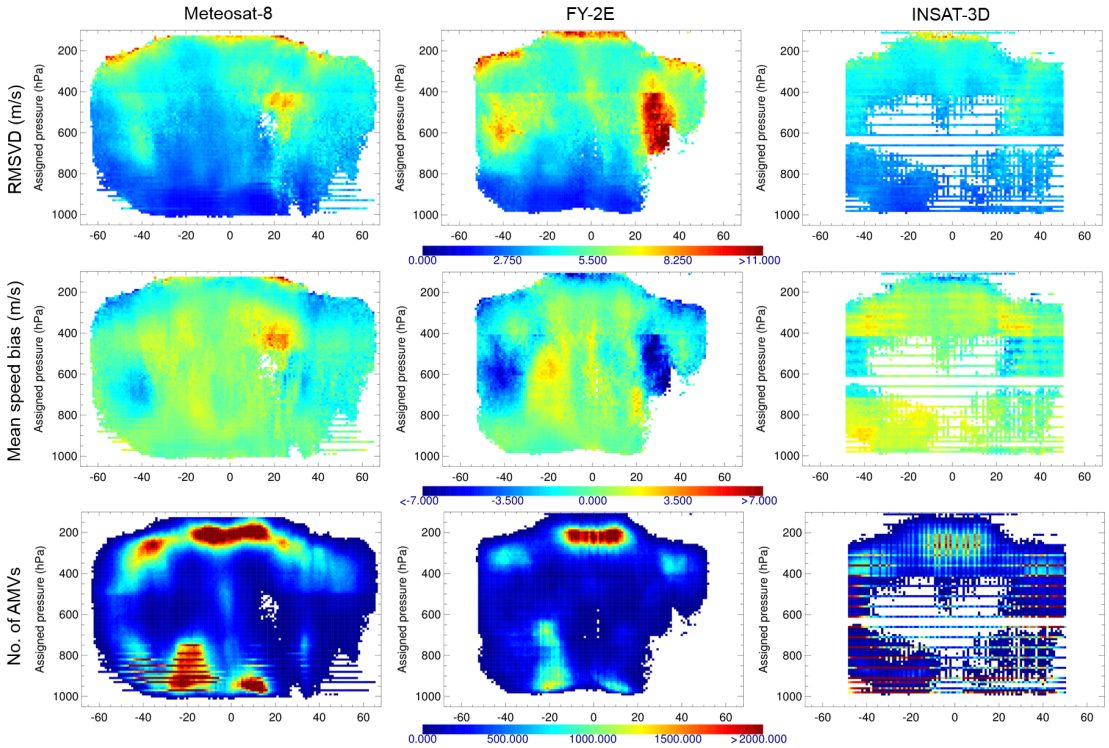

Figure 12: Zonal plots of RMSVD (top row), speed bias (middle row) and number of AMVs (bottom row) for Meteosat-8 (left), FY-2E (middle) and INSAT-3D (right) for the infrared channel from 1st Dec 2016 - 15th Jan 2017. For FY-2E and Meteosat-8 only AMVs with forecast independent QI > 80 are shown, all data are shown for INSAT-3D, a first guess check has been applied in all cases and only boxes with more than 20 AMVs are displayed.

dependence on these new QI values. However, for INSAT-3D the water vapour channel is left as a mixture of cloudy and clear sky winds while there is still no obvious trend in data quality with forecast independent QI. One slight difference to the previous study is that the number of INSAT-3D AMVs assigned a QI less than 50 was small when using the 2014 data, but has reduced to having almost no winds with these low values now. Although there are very few winds at low QI, it is difficult to assess whether data quality measures such as RMSVD are still without dependence. To guard against any undesirable effects, particularly if the data volume increased for these values in the future, a threshold of 50 might be sensible for longer term use of the data.

Zonal plots and maps of the AMVs have revealed differences in spatial density in addition to the variation in temporal coverage discussed in the previous section. Figure 12 and 13 show zonal plots of the RMSVD, speed bias and AMV density for the infrared and water vapour AMVs respectively on the three satellites as an example. Here FY-2E and Meteosat-8 have been screened using the first guess check and a forecast independent QI value of 80, which was chosen as an initial threshold to filter out many of the poorer quality observations while still maintaining a good number of observations (especially as it is being used in conjunction with the first guess check). The regular stripes in INSAT-3D are a result of the use of forecast data in the auto-editor step of the height assignment described earlier. For INSAT-3D the water vapour AMVs extend to higher pressures due to this mixture of clear (with peak sensitivity of the channels at higher pressures than the dense areas of high level AMVs) and cloudy situations. For FY-2E there appears to be an anomalous feature of many AMVs assigned around 150hPa. This is not realistic and also not present in the infrared channel.

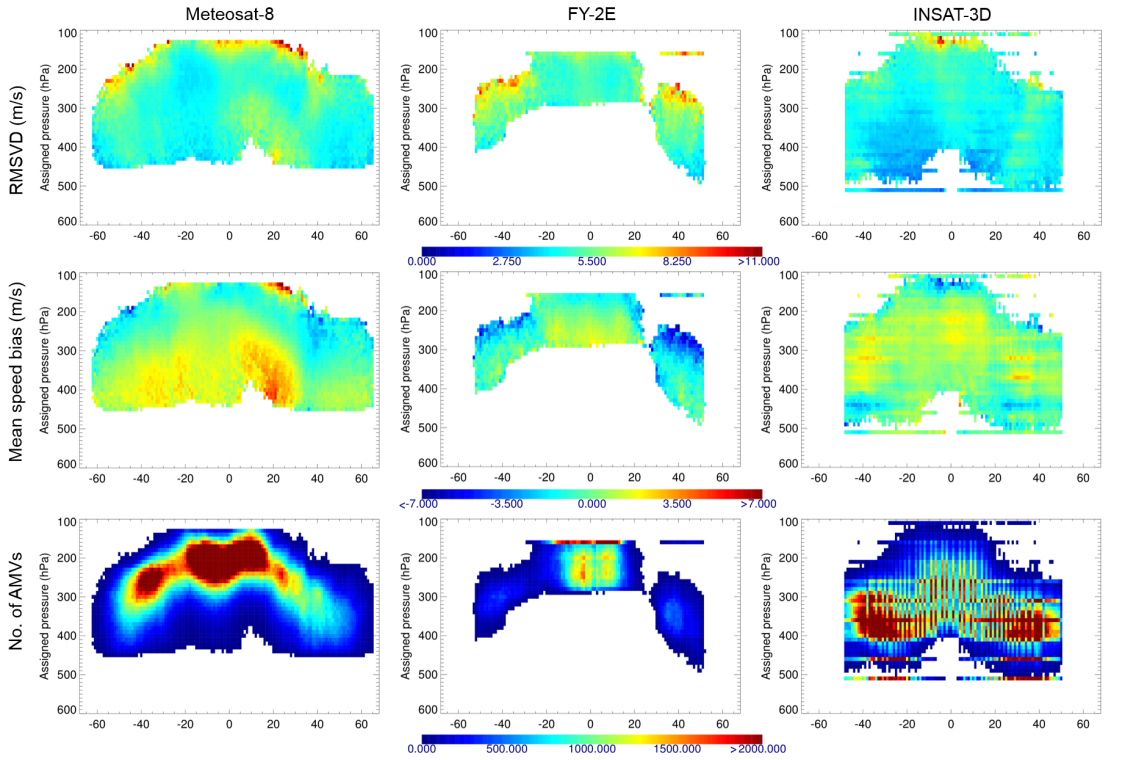

Figure 13: Zonal plots of RMSVD (top row), speed bias (middle row) and number of AMVs (bottom row) for Meteosat-8 (left), FY-2E (middle) and INSAT-3D (right) for the water vapour channel (6.25µm on Meteosat-8) from 1st Dec 2016 - 15th Jan 2017. For FY-2E and Meteosat-8 only AMVs with forecast independent QI > 80 are shown, all data are shown for INSAT-3D, a first guess check has been applied in all cases and only boxes with more than 20 AMVs are displayed.

Now the FY-2E water vapour AMVs have been separated the cloudy situation winds show much smaller speed biases in the tropics (around 2m/s compared to 6m/s for clear sky only (not shown)). High level AMVs for both Meteosat-8 and FY-2E show negative speed biases in the extra-tropics (figure 12, 13), although smaller in magnitude for Meteosat-8. As found in Salonen and Bormann (2015), INSAT-3D disagrees with slightly positive biases generally seen in the extra-tropics. For channels where low level winds (pressure $>$ 700hPa) are available, INSAT-3D has a slightly more positive speed bias, especially for the short-wavelength infrared channel where there is a relatively constant bias of 1-2m/s.

Figure 12 and 13 also demonstrate that, regardless of speed bias patterns, INSAT-3D generally shows similar or in many cases better agreement with the first guess. However, this is likely at the expense of independence from NWP. Further to this, despite the mixture of clear and cloudy water vapour winds the quality does not appear degraded compared to the cloudy only equivalent channels on the other satellites. Clear sky AMVs have not generally been used in the operational forecast system at ECMWF - traditionally the data quality has been worse than the cloudy AMVs and their inclusion during experimentation has caused negative impacts.

Earlier in figure 10 we saw that as well as different locations, the disc of FY-2E does not extend as far as Meteosat-8 while INSAT-3D has an artificial square shape due to the processing method. Global maps of the AMV numbers (not shown) reveal that broadly areas of dense AMVs are similar across the satellites but there are smaller areas of less agreement most likely due to the different derivation techniques and sensitivities of different wavelengths e.g. in water vapour.

7.1 Blacklisting choices and observation errors

Taking into consideration the first guess departure analysis, a set of satellite specific blacklisting choices were constructed for use prior to assimilation which are summarised in table 3. The aim was to make these as consistent as practical (e.g. by applying more conservative screening in the tropics), but different data characteristics meant that different quality control choices were inevitable in some areas (e.g. different QI thresholds tailored to the data quality variation). This screening is in addition to rejecting any AMVs with assigned pressures $>$ 500hPa over land, pressure more than 1000hPa or less than 100hPa globally and excluding AMVs at any height over most of the Northern Hemisphere land. This is an exploratory study so while the testing of different screening possibilities is not exhaustive, it should still provide good guidance on possible future paths.

The situation dependent observation errors for AMVs are calculated using contributions from two sources: the tracking error and error in speed due the error in height (Salonen and Bormann, 2013). Tracking errors are estimated using the standard deviations of the (observed - model background) wind speed for cases where the height error is small. The second part uses a combination of wind shear at the AMV location and height assignment error. Errors in the height assignment method are estimated using the standard deviation of the difference between assigned pressure and best-fit pressure (where the best-fit pressure is the model pressure that minimises the vector difference between the AMV and model wind e.g. Forsythe and Saunders (2008)). For both parts of the error calculation, values are generated for 200hPa layers from 1000 to 100hPa. In practice, the same tracking errors are currently used across all geostationary satellites which vary between 2 and 3m/s depending on height. Considering the relevant statistics outlined above, for all the IODC satellites, these values are still sensible even despite the lower precision of the FY-2E wind speeds.

Using the blacklisting choices outlined in table 3 the data were screened before calculating the best-fit pressure statistics required for the height assignment error estimate. Figure 14 illustrates the (assigned

Table 3: Blacklisting choices for Meteosat-8, FY-2E and INSAT-3D. (IR = Infrared, SWIR = Short wavelength IR, Vis = Visible, WV = Water Vapour, QI refers to forecast independent type.)

Channel	Meteosat-8	FY-2E	INSAT-3D
All channels	QI $<$ 85	QI $<$ 85	QI $<$ 50
Vis	P $\leq$ 700hPa, QI $\leq$ 85	not available	P $\leq$ 700hPa
WV	|Lat| $<$ 25 and P $>$ 250hPa, WV(6.25μm): P $>$ 400hPa, WV(7.95μm): P $>$ 600hPa	160hPa $<$ P $<$ 400hPa, |Lat| $>$ 25 and QI $<$ 90	P $>$ 500hPa (P $>$ 250hPa for assimilation)
IR	|Lat| $<$ 25 and P $>$ 250hPa	|Lat| $<$ 25 and 400hPa $<$ P $<$ 700hPa |Lat| $>$ 25 and QI $<$ 90	|Lat| $<$ 25 and P $>$ 400hPa
SWIR	Not available	Not available	P $\leq$ 700hPa

- best-fit) pressure bias, standard deviation and number of AMVs for each 200hPa layer considered for the infrared channel on each satellite. While in the top two layers 0-400hPa the results are quite similar between all three satellites, at mid and lower levels, INSAT-3D performs better with lower standard deviation and bias values. FY-2E in particular has large biases 400-800hPa (more than 100hPa) compared to INSAT-3D and Meteosat-8. These are reduced by 30-40hPa after application of the first guess check but still remain comparatively large. In the best-fit pressure statistics the tropics and mid-levels tend to be the poorest quality areas for each of the satellites. The water vapour channels also show similar results, even with the mixture of clear and cloudy situations in INSAT-3D. In the visible channel, Meteosat-8 and INSAT-3D share similar standard deviations of around 110-130hPa while the low level winds of the shortwave infrared are more in line with the longwave infrared channel, at around 140-160hPa.

8 Assimilation of IODC satellites

With the promising results in the data quality analysis, the next step is to run assimilation experiments to test the longer term impact of the data on the forecast system. For this part of the assessment, a control was run which mimics the operational system at that time (cycle 43r1) but at a lower resolution of $T_{Co}399$ (55km). A further change is the removal of the geostationary satellite providing IODC. Each IODC satellite was then introduced in isolation and in addition to testing the AMVs, experiments considering the ASRs from Meteosat-8 were also conducted in order to investigate the complete impact of the IODC service. Due to the restrictions on the availability of the AMV data and the requirement for experiments with radiance data to have at least a month of processing to allow the variational bias correction to reach stability, verification statistics have been calculated for 1st Dec 2016 - 30th June 2017.

Early results quickly showed unexpected negative impacts in the INSAT-3D experiments. The fit of humidity sensitive observations was consistently and often significantly degraded across both microwave and infrared sounding instruments such as ATMS and Infrared Atmospheric Sounding Interferometer

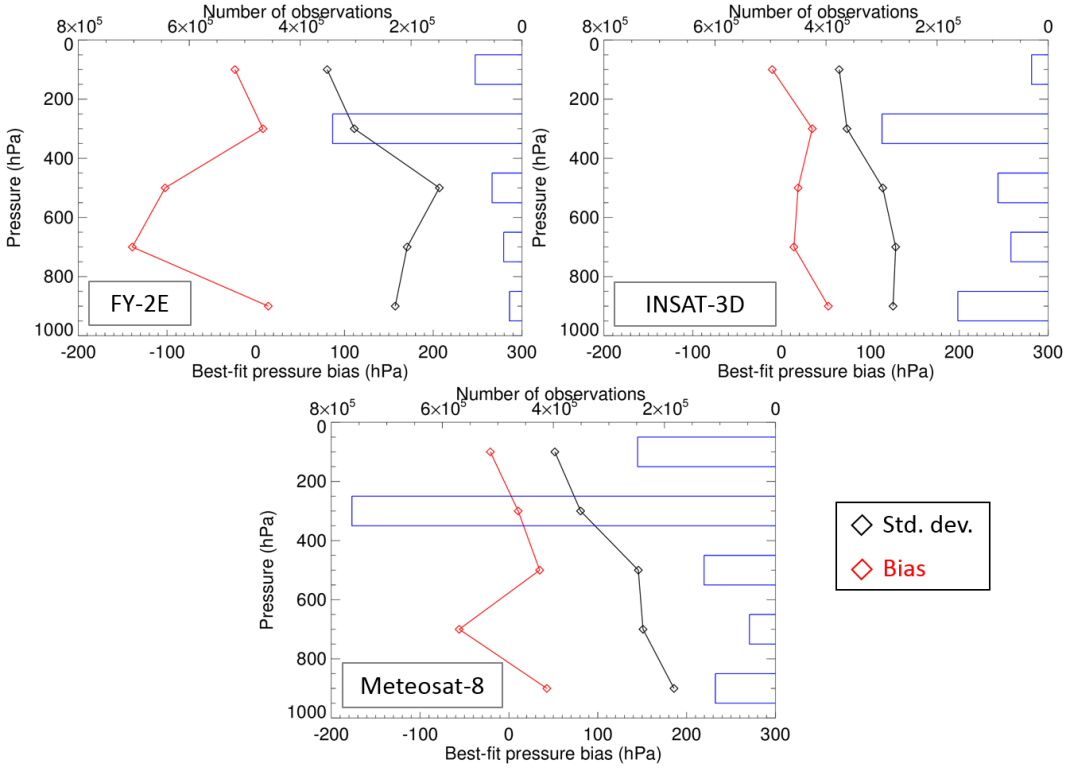

Figure 14: Assigned - best-fit pressure bias and standard deviation for each 200hPa band for the longwave infrared channel on FY-2E (top left), INSAT-3D (top right) and Meteosat-8 (bottom). Bars show the number of observations. Values are calculated from data that has been screened using the suggested blacklisting choices in table 3 and calculated for 1st Dec 2016 - 15th Jan 2017.

(IASI). A small degradation ($\sim$0.4%) around 500hPa was also present for the conventional wind observations in the tropics. Further to this, in the verification against own analysis, there was an area of negative impact in the region of the INSAT-3D coverage at 500hPa. The use of INSAT-3D alone introduces a large increase in the global total number of AMVs used in the 300-500hPa varying between about 30-50%. It is likely that a large portion of the AMVs assigned lower mid-range pressures originate from clear-sky scenes which are not distinguished from cloudy scenes for the INSAT-3D AMVs. In a simple attempt to remove many of these clear sky AMVs, a more conservative limit was applied to the water vapour channel which restricted winds to pressure $<$ 250hPa. This very effectively removed the negative impacts detailed.

The following list is the final set of experiments:

1. Meteosat-8 AMVs
2. INSAT-3D AMVs (with added rejection of pressure $>$ 250hPa for water vapour channel)
3. FY-2E AMVs
4. Meteosat-8 ASRs
5. Meteosat-8 AMVs and ASRs

The inter-comparison of the AMV only experiments is discussed in the following section. The impact of the additional ASRs will be considered separately in section 8.2.

8.1 AMV impacts

While the total number of AMVs available in the received files is highest for Meteosat-8, below 250hPa INSAT-3D generally has a higher number of observations actively assimilated (up to twice as many as Meteosat-8 at 400hPa in the tropics) (figure 15). This is due to a combination of more relaxed blacklisting but also better agreement with the model background means that a lower percentage of winds are removed during the first guess check quality control step. FY-2E generally adds the fewest new observations with less than 5% change to the global total compared to 10-20% for the other satellites.

Despite the differences in data numbers and first guess departures discussed earlier, the impacts of the three satellites were surprisingly similar. When verifying with the fit of independent observations, changes over larger areas are mostly neutral for FY-2E and INSAT-3D as was also seen in the Meteosat-7/8 comparison. Focusing only on the region covered by the IODC satellites as before, the impact is a little more significant as illustrated in figure 16. Here in the V component of the PILOT winds all three satellites show a significant reduction in the fit to the model background while the changes are neutral for the U component of the radiosondes. This also demonstrates the similarity in the short-range forecast impact between the satellites.

In the verification against own analysis, the high levels show positive impacts, more significant for INSAT-3D and FY-2E, localised over the tropical Indian Ocean (figure 17). At lower levels there are also some reductions in error, particularly for INSAT-3D to the south of the equator. The degradation feature in Meteosat-8 at 850hPa (first mentioned in section 3.2.1) is not apparent in the other satellites - part 3 of this report is dedicated to discussion of this challenging area.

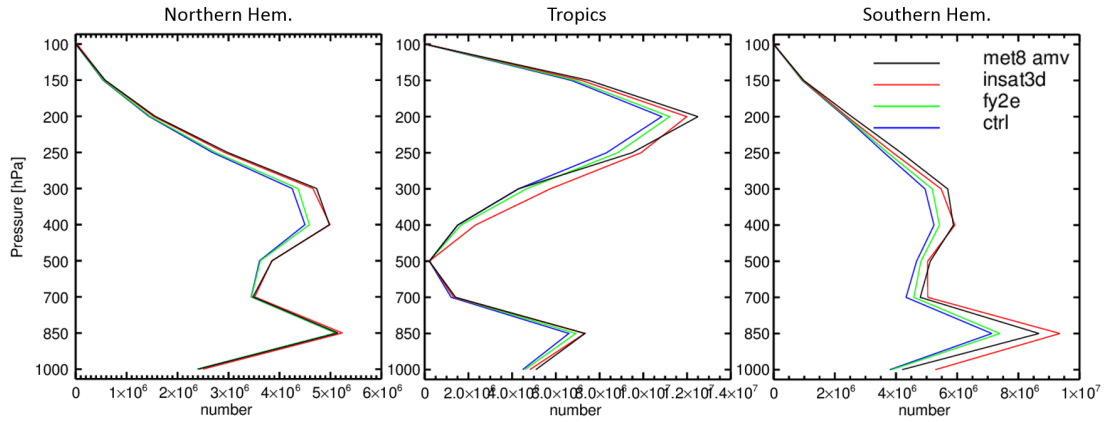

Figure 15: Total number of AMVs at varying pressure levels with the addition of each IODC satellite for the Northern Hemisphere (left), Tropics (middle) and Southern Hemisphere (right). Data from 1st Dec 2016 - 30th Jun 2017.

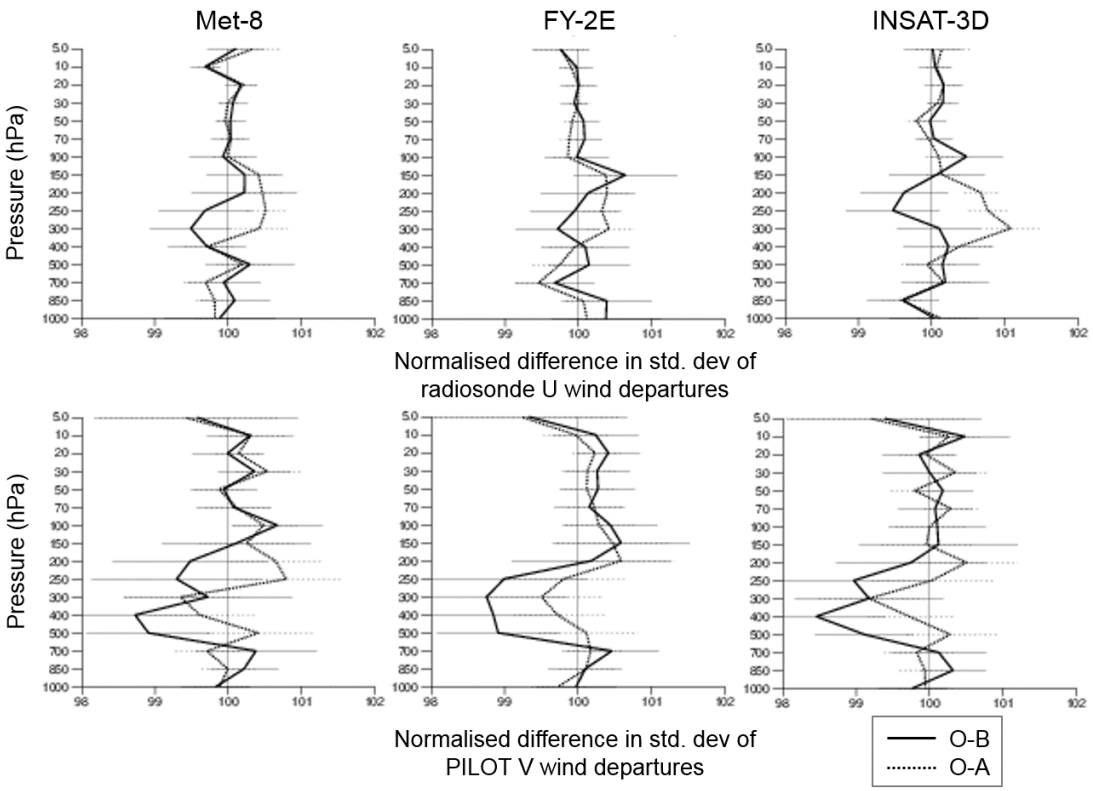

Figure 16: Change in standard deviation of observation departure from background/analysis for the U component of radiosonde winds (top row) and V component of PILOT winds (bottom row) in the experiment assimilating Meteosat-8 (left), FY-2E (middle) and INSAT-3D (right). Data from 1st Dec 2016 - 28th Feb 2017 over the Indian Ocean region only (60°N-60°S, 30-120°E).

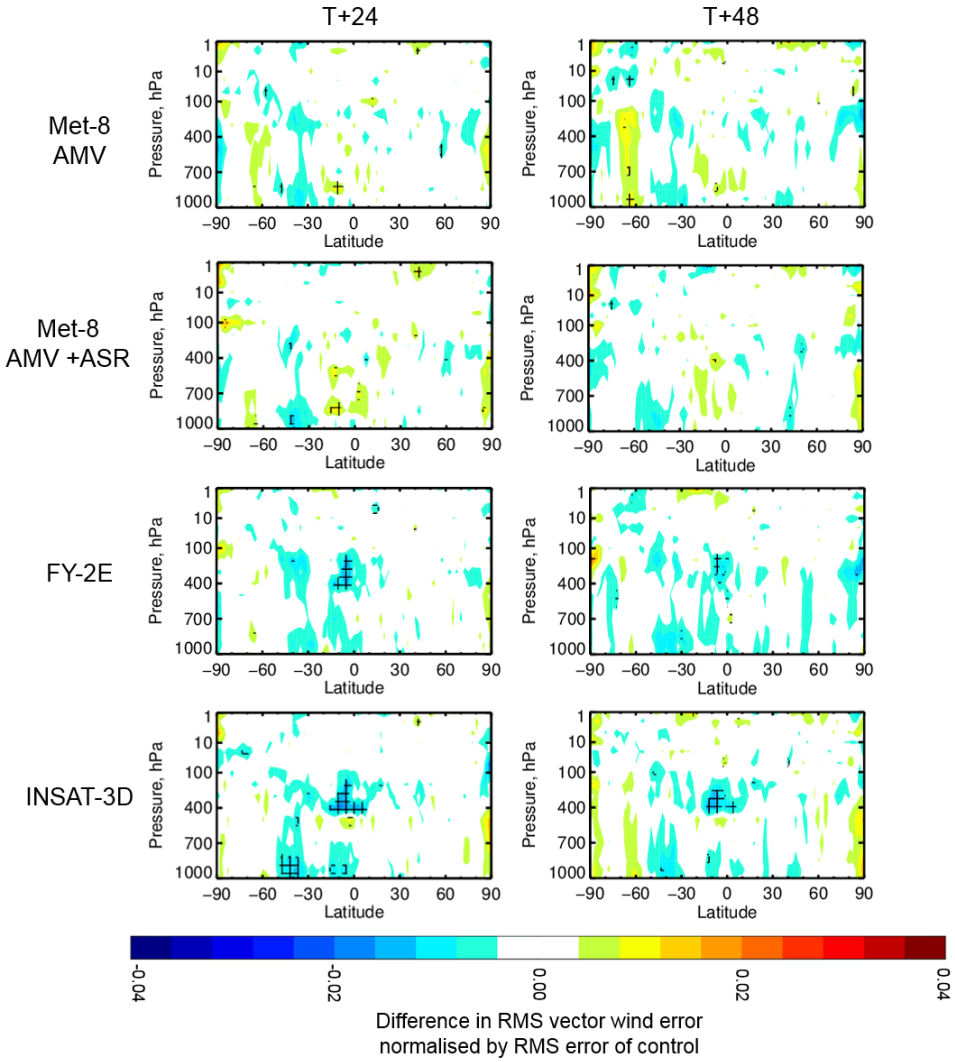

Figure 17: Zonal plots of the change in vector wind error verified against own analysis for the 24 (left column) and 48 (right column) hour lead times for Meteosat-8 AMV only (top row), Meteosat-8 AMV and ASR (second row), FY-2E (third row) and INSAT-3D (bottom row). Data from 1st Dec 2016 - 30th Jun 2017. Black hatched lines indicate significance at the 95% level.

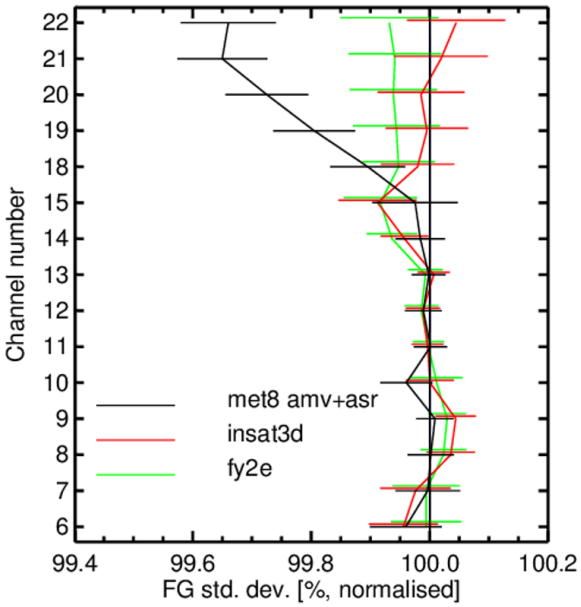

Figure 18: Change in standard deviation of observation departure from background for ATMS for the experiments assimilating Meteosat-8 AMV and ASR while AMV only for FY-2E and INSAT-3D. Channels 18-22 are the tropospheric humidity sounding channels. Data from 1st Dec 2016 - 30th Jun 2017 over the global area.

8.2 AMV and ASR

Typically the assimilation of the water vapour channel radiances has greatest impact on humidity and related fields. The AMVs from the IODC satellites showed very little influence on the humidity fields. It is very clear that in the IODC, the ASR product provides added benefit in the fit of independent humidity sensitive observations compared to AMVs alone on INSAT-3D or FY-2E (figure 18). The effects are large enough that the reduction in standard deviation is clear even when verifying over a much larger area than earlier for the AMVs.

Additionally, through the 4D-Var tracing effect it is possible to positively influence the winds fields through the assimilation of ASRs (Peubey and McNally, 2009). Focusing on verification over the Indian Ocean area, when adding Meteosat-8 ASR only (no AMVs) the impacts on the independent conventional wind observations are neutral (not shown). This is a smaller, indirect effect and large areas of overlap with the adjacent geostationary satellites mean that small changes are not necessarily surprising. Figure 17 shows only small changes between the experiments with AMVs alone and with the addition of ASR. However, when verifying the combination of AMV and ASR against the Meteosat-8 AMV only experiment in place of the control, at longer lead times (two - five days) the verification against own analysis (not shown) reveals small but significant improvement in the vector wind error around 40-60°S throughout the troposphere.

9 Summary

The relative benefits and limitations of three different satellites providing coverage of the Indian Ocean have been investigated. Variation in the different imaging instruments and AMV derivation methods result in large differences in the number of AMVs available and their distribution. This also followed through to differences in the data quality assessed by first guess departures. INSAT-3D showed consistent and closer agreement with the model background but there is more dependence on NWP in the derivation. The spatial patterns of the statistics were also varied with similarity between Meteosat-8 and FY-2E such as negative speed biases in the high-level extra-tropics while INSAT-3D exhibited slightly positive biases in the same region.

Although there were significant differences between the AMV characteristics, assimilation experiments showed similar results. All three satellites demonstrated benefit in the vector wind field over the tropics and showed slight improvements in the fit of independent conventional wind observations. To understand the full impact of the IODC in the forecast system the ASR product, available only from Meteosat-8 at present, was also considered. There were clear and significant benefits in the fit of independent humidity sensitive observations to the first guess while changes in the wind fields and fit of wind observations were mostly small and neutral.

At present, no changes are planned to the use of Meteosat-8 over the Indian Ocean. Improvements to FY-2E, such as adding the forecast independent QI and separating the clear and cloudy water vapour winds, have led to better quality AMVs in assimilation and more benefit than recorded in the earlier study by Salonen and Bormann (2015). However, in first guess departures and observation errors, Meteosat-8 generally provides better statistics than FY-2E. Despite promising departure statistics, the clear sky water vapour winds included for INSAT-3D produced negative impacts when assimilated. Once many of these winds were removed, INSAT-3D showed positive or neutral results comparable to the other satellites but in future, it would be useful if the cloudy and clear sky situations were separated. Also, time series of the data volume revealed less reliability in the number of AMVs and occasional outages in the INSAT-3D data. For any potential future IODC satellites, the added benefit of the ASR product is also important. It would be interesting to consider FY-4A, with a more advanced imaging instrument than FY-2E, when AMV data become available (although with a similar location to FY-2G the gap between Himawari-8 and Meteosat-10 may not be so completely covered). Also the introduction of the first infrared hyperspectral sounding instrument on FY-4A presents an exciting development in the direct assimilation of radiances.

Part III

Challenges at 850hPa

This final part of the report revisits the area of apparent degradation seen in a localised area over the Indian Ocean in the Meteosat-8 experiments when verification against own analysis is considered. The challenge is to identify how much this degradation can be attributed to the AMVs, if this is a model based problem or even a verification problem. Since initial discovery of the feature during the switch from Meteosat-7, the longer experimentation run for the IODC satellite inter-comparison has provided the opportunity for a more in depth investigation. In running the set of IODC experiments, it is clear that both INSAT-3D and FY-2E do not show a corresponding area of degradation (figure 19). Also, with a longer experiment time, the feature in Meteosat-8 has not significantly reduced. When verified using

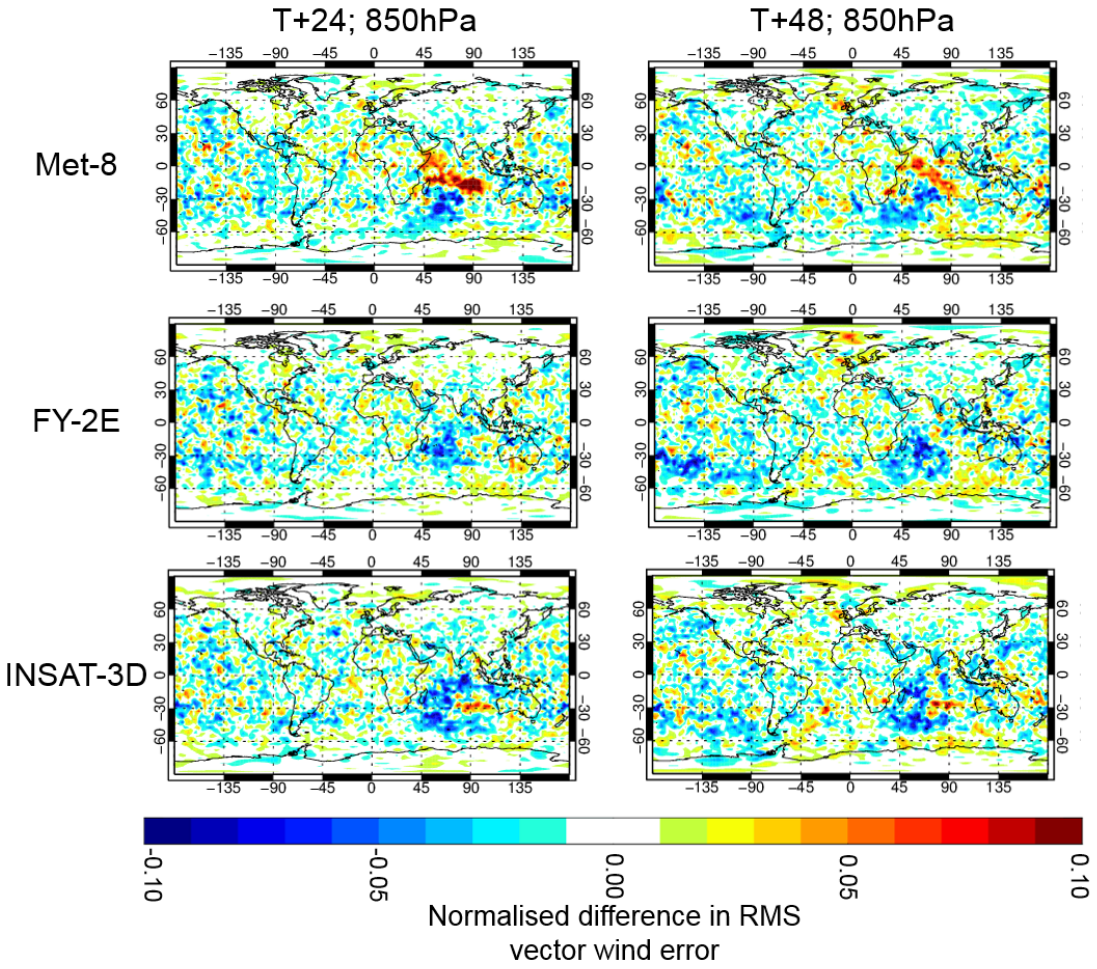

Figure 19: Change in vector wind error at 850hPa at forecast lead time T+24 and T+48 for Meteosat-8 (left), FY-2E (middle) and INSAT-3D (right). Forecasts are verified against own analysis for 1st Dec 2016 - 30th Jun 2017.

the operational analysis as a reference (which assimilated Meteosat-7) there is a degradation in the T+12 forecast in the affected area but at subsequent forecast times the verification returns to neutral. This suggests that the Meteosat-8 AMVs are increasing the variance of the analysis which persists into the very short range forecast. As a consequence, degradation against own analysis at lead times of T+24 and beyond may not necessarily be indicating a problem in the forecast but instead reflect a more variable reference field. This result also indicates that the presence of the degradation in the forecast is sensitive to the verifying analysis.

In the initial Meteosat-8 experiment from part 1, this signal at 850hPa actually starts off much stronger in the early weeks of the experiment and then lessens as the period becomes longer into February/March. Earlier in section 3.2.1, figure 9 showed that there are also changes to the mean wind analysis through assimilation of the Meteosat-8 AMVs. In the Indian Ocean there is a general westward flow which is strengthened by the addition of the AMVs. This effect is also seen but more weakly with the Meteosat-7 data. Examination of the mean change in the forecast U component of the wind over the longer experiment period (figure 20) shows that the addition of the AMVs for all three satellites actually has a

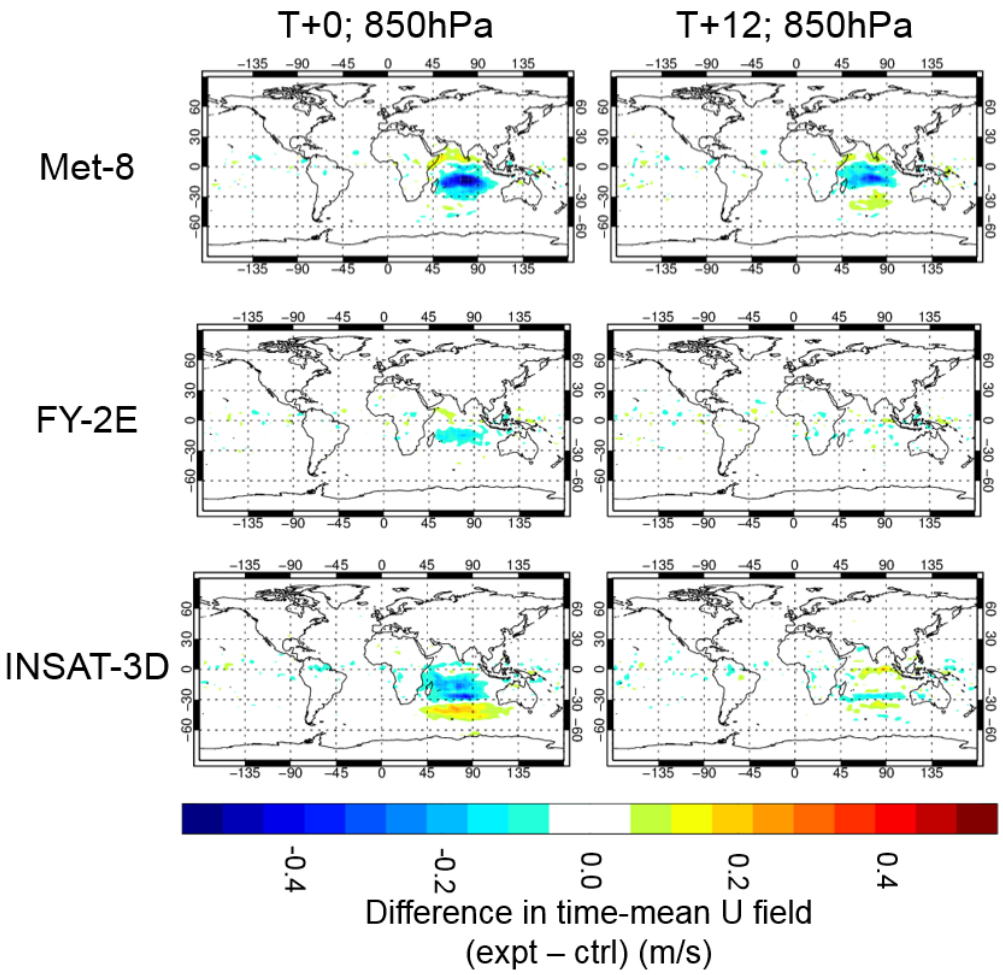

Figure 20: Change (experiment - control) in U component of mean wind field at 850hPa at analysis time and forecast lead time T+12 for Meteosat-8 (top), FY-2E (middle) and INSAT-3D (bottom). Data are for 11th Dec 2016 - 30th Jun 2017.

consistent effect on the analysis of increasing the zonal wind in the tropics in a similar region. However, for Meteosat-8 this change is much larger (around 0.5m/s compared to 0.2m/s for INSAT-3D) and the feature persists into the T+12 forecast whereas INSAT-3D and FY-2E show no change even at this short forecast range. After this initial change applied at the analysis time, the influence of the Meteosat-8 AMVs does not propagate far into further forecast lead times i.e. the experiment with Meteosat-8 and the control quite quickly converge to the same forecast wind field.

10 Identifying model bias

Figure 21 considers the change in mean forecast error of the U wind component (difference between forecast and analysis) at day 1, 2, 5 and 10 for the early part of the experiment with Meteosat-8. The red colours in the area to the south of India, coinciding with the region of degradation seen in the verification,

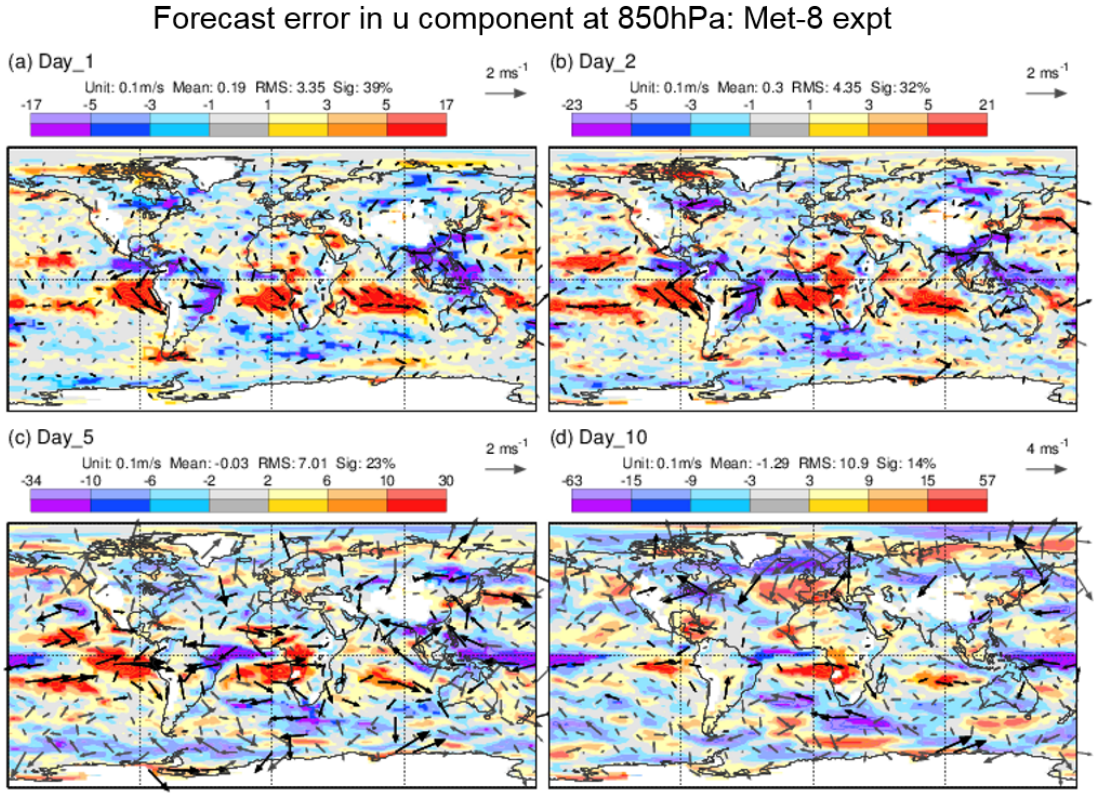

Figure 21: Maps showing the mean forecast error (forecast - analysis) in the U wind component for increasing forecast lead times calculated using data from the experiment including Meteosat-8 AMVs (data from 1st Nov 2016 - 15th Jan 2017). Bolder colours indicate 95% significance.

indicate that the westward flow in the forecast is too slow compared to the analysis. This bias increases as the forecast lead time increases - it approximately doubles over the 10 day period. This is suggestive of a model problem. Performing the same analysis on the control run and hence using an analysis that has not assimilated AMVs in this region (not shown) still shows this model bias so it is not (only) a feature caused by a biased analysis. In the control, the wind will be inferred indirectly from other observations, linking humidity and temperature observations through 4D-Var to changes in the wind field.

Previously it was noted that the Meteosat-8 AMVs change the analysis to strengthen the wind field but this effect does not persist long into the forecast. This means that we have wind forecasts from experiment and control that converge relatively quickly (by T+72) that both exhibit the characteristic of an increasing model bias that slows the winds. However, we are verifying against different analyses where the winds are faster in the analysis when Meteosat-8 is included. This will make the error appear larger for the Meteosat-8 experiment when compared to the control. While we cannot say that the AMVs are not contributing to the error, the evidence presented here points to model bias being at least partly responsible for the signal and AMVs from the other satellites support making these winds faster in the analysis.

For late January - March, analysis of the forecast error does not show this model bias and the verification no longer has this strong degradation feature. A Hovmöller plot (December-June) of the profiles of the low level model winds sampled at the AMV locations in the affected area was produced (not shown) and

this revealed that during February in particular there was a different wind flow in the region of interest. Generally the low level winds here flow in a westward direction but the regime changed temporarily to an eastward direction. By breaking up the verification into shorter time periods, it was found that after the weakening in January - March, the Meteosat-8 AMVs again exert a relatively large change to the mean wind analysis in the region in spring, which also extends up the coast of East Africa. This seems to translate once more into degradation in the verification however, the signs of model bias do not appear to be present for these spring months.

11 Profiles of low level winds

The possibility of AMV biases has also been investigated. To better understand the structure of the low level AMVs, vertical profiles of the wind speed and number density were studied using data only from a box covering the affected area (50-100°E, 5-25°S). Figure 22 shows statistics for the U component of the wind which has a very similar pattern for Meteosat-8 and FY-2E. The AMV wind profile shows very little variation in height for both cases while the model winds, sampled at the AMV locations of the respective satellites, suggests more wind shear. INSAT-3D agrees more with the model however this is likely due to the increased NWP dependence in the derivation process. Spikes in the profiles of Meteosat-8 correspond to inversion levels where many more AMVs are assigned, as shown in the number density plots. Although displaying agreement with Meteosat-8, FY-2E has comparatively very few winds in the region which may have resulted in any signal being too weak to show in the verification. Similar profiles were also generated (not shown) from an ocean region at higher latitudes and these showed closer agreement in variation of the AMVs and model confirming that this discrepancy is not a feature for all low level AMVs.

Unfortunately, this area of the ocean is very sparsely covered by conventional wind observations. Profiles from two radiosonde sites (Cocos Island and Réunion Island) on the periphery of the affected area were considered and these both supported some variation with height. This suggests that the AMVs might have a height assignment error where the faster winds are being placed too high or that the height assignment cannot reliably distinguish different levels between 700 and 950hPa. However, it is clear that this is also a challenging region for the model so we should be cautious about placing too much trust in these values. The inclusion of the AMVs may still have a positive influence in an otherwise poorly constrained area for wind.

12 Conclusions and future work

During the experimentation in the switch from Meteosat-7 to Meteosat-8, a degradation feature was identified in a localised area of the Indian Ocean. A model bias was identified for the early part of this experiment where the forecast winds are too slow compared to the analysis. The AMVs act to increase the wind speed of the analysis but this effect does not propagate far into the forecast leading to an increase in error when verifying the experiment against its own analyses. With the benefit of a longer experimentation period during the comparison with other IODC satellites, it appeared that this degradation continued in the spring months while the model bias seems to disappear.

Despite their different characteristics, each IODC satellite acts to strengthen the westward wind flow but Meteosat-8 has significantly more AMVs in the region which enhances the signal. Profiles of the Meteosat-8 and FY-2E AMVs showed little wind shear in the area while the model, sampled at the AMV

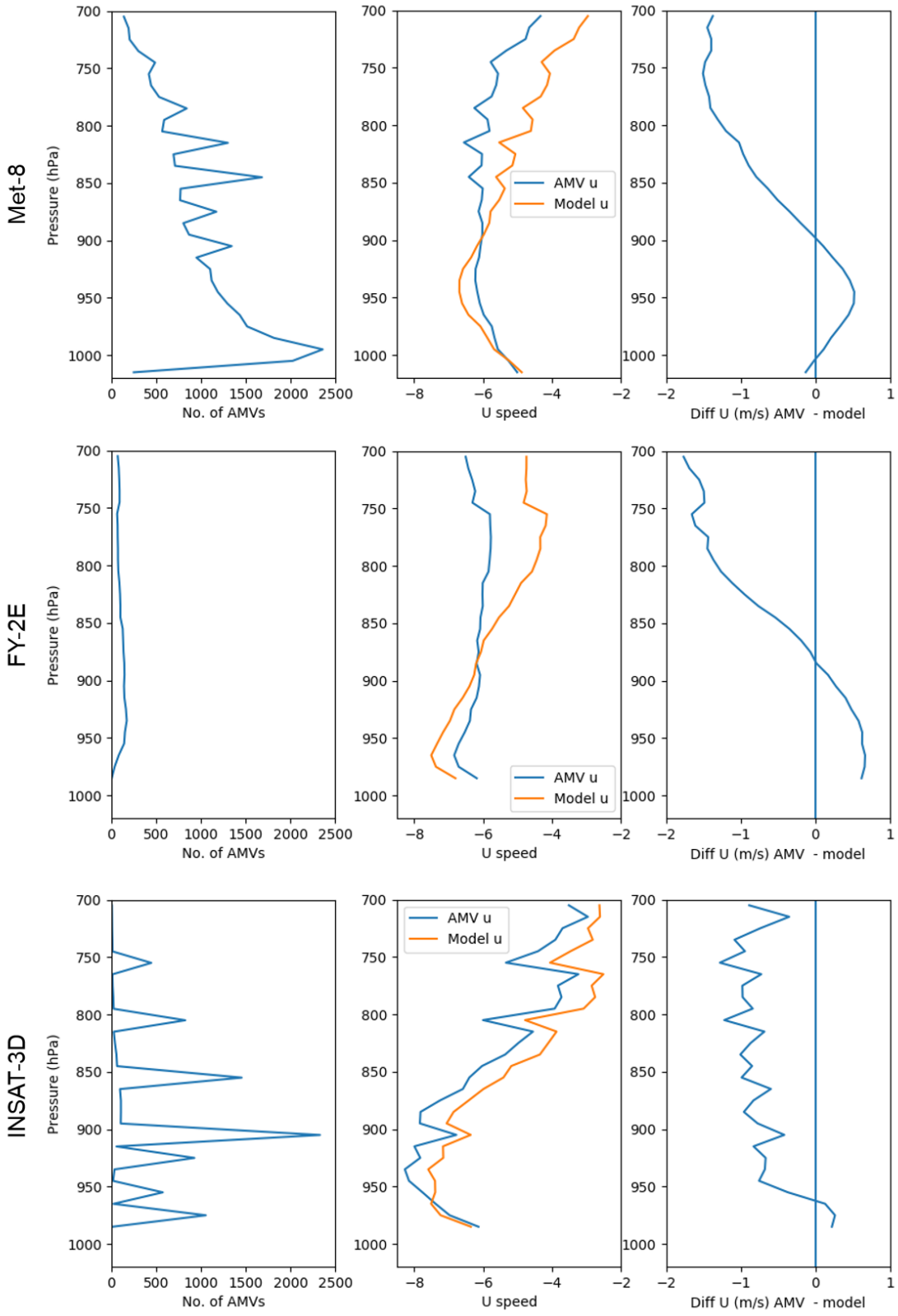

Figure 22: Mean of the daily profiles of number of observations (left column), U component of wind for AMV and model wind sampled at AMV locations (middle column) and U bias (right column) using data for Meteosat-8 (top row), FY-2E (middle row) and INSAT-3D (bottom row). Data are from both infrared and visible channels (where available), within the box extending 50-100°E, 5-25°S, screened by QI and first guess check, for the period 1-31st Dec 2016 and compared to a background where no IODC AMVs had been assimilated.

locations, suggested more variation with height. A lack of conventional observations made independent verification difficult although nearby radiosondes also pointed towards a profile with more variation than displayed in the AMVs.

A possible explanation is that the AMVs are assigned too high. Since it is a difficult area for the model and conventional observations are sparse, other routes to gaining information about the AMVs could include comparing the cloud heights to Cloud-Aerosol Lidar and Infrared Pathfinder Satellite Observation (CALIPSO). Winds derived from the Multiangle Imaging SpectroRadiometer (MISR) using a stereoscopic method may also give some insight into the heights and provide further information about the typical wind shear. In the future, ADM-Aeolus will also allow assessment of the area with an independent source. For now, without firm evidence for the truth, the use of the low level Meteosat-8 winds remains unchanged with the aim of providing some useful constraint on the model wind field.

Acknowledgements

Katie Lean is funded by the EUMETSAT Fellowship Programme.

References

Deb, S., 2012. Multiplet based technique to derive atmospheric winds from Kalpana-1. Proceedings of the 11th International Winds Workshop, Auckland, New Zealand, 20-24 February 2012.

Deb, S., Sankhala, D. K., Kishtawal, C. M., 2016. Atmospheric Motion Vectors from INSAT-3D: ISRO status. Proceedings of the 13th International Winds Workshop, Monterey, California, 27th June - 1st July 2016.

Forsythe, M., Saunders, R., 2008. AMV errors: a new approach in NWP. Proceedings of the 9th International Winds Workshop, Annapolis, Maryland, USA, 14-18 April 2008.

Holmlund, K., 1998. The utilization of statistical properties of satellite-derived atmospheric motion vectors to derive quality indicators. Wea. Forecasting 13, 1093–1104.

Lean, K., Bormann, N., Salonen, K., 2016. Assessment of Himawari-8 AMV data in the ECMWF system. EUMETSAT/ECMWF Fellowship Programme Research Report No.42.

Letertre-Danczak, J., In progress. Aerosol content from hyperspectral infrared sounders and improvement in geostationary radiance observation assimilation at ECMWF: final report. EUMETSAT/ECMWF Fellowship Programme Research Report.

Lupu, C., McNally, A., 2014. Impact assessment of GOES-15 CSR and Meteosat-10 ASR in the ECMWF system. EUMETSAT/ECMWF Fellowship Programme Research Report. No.33.

Menzel, W., P., Smith, W., L., Stewart, T., R., 1983. Improved cloud motion wind vector and altitude assignment using VAS. J. Climate Appl. Meteor 31, 370–384.

MSG Meteorological Products Extraction Facility Algorithm Specification Document, October 2015. Eum/msg/spe/022, v7b draft Edition.

Nieman, S., J., Schmetz, J., Menzel, W., P., 1993. A comparison of several techniques to assign heights to cloud tracers. J. Appl. Meteor. 32, 1559–1568.

Payan, C., Rabier, F., 2004. The use of Meteosat winds with Quality Indicators within the Météo-France Global NWP Model. Proceedings of the 7th International Winds Workshop, Helsinki, Finland, 14-17 June 2004.

Peubey, C., McNally, A., 2009. Characterization of the impact of geostationary clear-sky radiances on wind analyses in a 4D-Var context. Q. J. R. Meteorol. Soc. 135, 1863–1876.

Salonen, K., Bormann, N., 2013. Winds of change in the use of Atmospheric Motion Vectors in the ECMWF system. ECMWF Newsletter 136, 23–27.

Salonen, K., Bormann, N., 2015. Atmospheric Motion Vector observations in the ECMWF system: Fourth year report. EUMETSAT/ECMWF Fellowship Programme Research Report No.36.

Szejwach, G., 1982. Determination of semi-transparent cirrus cloud temperature from infrared radiances: Application to meteosat. Journal Appl. Meteor. 21, 384–393.

Velden, C. S., Olander, T. L., Wanzong, S., 1998. The impact of mulispectral GOES-8 wind information on Atlantic tropcial cyclone track forecasts in 1995. Part I: Dataset methodology, description and case analysis. Monthly Weather Review 126, 1202–1218.

Xu, J., Holmlund, K., Zhang, Q., Schmetz, J., 2002. Comparison of two schemes for derivation of atmospheric motion vectors. J. Geophys. Res. (D14), ACL 4–1–ACL 4–15.

Zhang, X., Xu, J., Zhang, Q., 2016. Status of operational AMVs from Fengyun-2 satellites. Proceedings of the 13th International Winds Workshop, Monterey, California, 27th June - 1st July 2016.